



**RESEARCH DEPARTMENT**

---

**Image orthicon investigations:  
the discharge of the target  
by the beam**

**RESEARCH REPORT No. T-100/4**

**1964/37**

**THE BRITISH BROADCASTING CORPORATION  
ENGINEERING DIVISION**

RESEARCH DEPARTMENT

**IMAGE ORTHICON INVESTIGATIONS : THE DISCHARGE OF THE  
TARGET BY THE BEAM**

Research Report No. T-100/4

(1964/37)

C.R.G. Reed, M.A., A.M.I.E.E.  
J.R. Sanders, M.A.

*D. Maurice*

(D. Maurice)

This Report is the property of the  
British Broadcasting Corporation and  
may not be reproduced in any form  
without the written permission of the  
Corporation.

## CORRIGENDA

RESEARCH DEPARTMENT - BRITISH BROADCASTING CORPORATION

Research Report No. T-100/4 (1964/37)

*IMAGE ORTHICON INVESTIGATIONS :  
THE DISCHARGE OF THE TARGET BY THE BEAM*

Page 24 Fig. 18, scale of abscissa: delete ' $\text{metres/sec}^{-1}$ ', insert ' $\text{metres.sec}^{-1}$ '.

Page 25 Fig. 19, scale of abscissa: delete ' $\text{metres/sec}^{-1}$ ', insert ' $\text{metres.sec}^{-1}$ '.

Page 28 Section 6, line 2: delete '10(c)', insert '10(b)'.

Page 28 Section 6, line 3: delete 'equiangular'.

Page 29 End of first paragraph, insert:

'The waveforms are those obtained during selected lines that cross the image of the moving patch. The scale indicates the time, since illumination began, at which the left-hand (trailing) edge of the patch reached any given position along the line'.

Page 34 Paragraph beginning line 3: delete second sentence.

# **IMAGE ORTHICON INVESTIGATIONS : THE DISCHARGE OF THE TARGET BY THE BEAM**

Section	Title	Page
	SUMMARY . . . . .	1
1.	INTRODUCTION . . . . .	1
2.	THE PROCESSES OF CHARGING AND DISCHARGING THE TARGET . . . .	1
2.1.	The Process of Charging the Target . . . . .	2
2.2.	The Process of Discharging the Target . . . . .	4
2.2.1.	The Effect of the Initial Potential of the Target on Discharge Efficiency . . . . .	6
2.2.2.	The Effects of a Change in Beam Current on Discharge Efficiency . . . . .	9
2.2.3.	The Influence of the Focus and Deflection Systems on Target Discharge . . . . .	10
2.2.4.	Discharge of the Target when the Width of a Scanned Line is Equal to the Spacing of Lines in a Field . . . .	11
2.2.5.	Discharge of the Target when the Width of a Scanned Line is Equal to the Spacing of Lines in a Picture . . .	13
2.2.6.	The Differences Between the Effects of Intermittent and Continuous Illumination of the Photo-Cathode . . . . .	13
3.	DESCRIPTION OF THE APPARATUS . . . . .	14
4.	EXPERIMENTAL METHOD USED FOR INVESTIGATION OF TARGET DISCHARGE . . . . .	15

Section	Title	Page
5.	EXPERIMENTAL RESULTS . . . . .	15
5.1.	Factors Investigated in order to Ascertain Their Effects on the Discharge of the Target . . . . .	15
5.2.	The Effects of the Beam-Focus and Target Mesh Potentials on the Discharge of the Target . . . . .	16
5.3.	The Effect of Beam Current on the Discharge of the Target . .	17
5.4.	The Effect of Target Temperature on the Discharge of the Target . . . . .	18
5.5.	The Effect of Illumination Level on the Discharge of the Target . . . . .	20
5.6.	The Efficiency of Target Discharge as a Function of the Type of Scanning Raster Used . . . . .	21
5.7.	The Effect of Line Scan Velocity on the Discharge of the Target . . . . .	23
5.8.	The Effect of Line Spacing on the Discharge of the Target . .	24
6.	THE PORTRAYAL OF A MOVING OBJECT . . . . .	28
7.	CONCLUSIONS . . . . .	33
8.	REFERENCES . . . . .	34
	APPENDIX 1 . . . . .	36
	APPENDIX 2 . . . . .	43

June 1964

Research Report No. T-100/4

(1964/37)

## **IMAGE ORTHICON INVESTIGATIONS : THE DISCHARGE OF THE TARGET BY THE BEAM**

### **SUMMARY**

The measurements described in this report were carried out in order to examine the mechanism and characteristics of the discharge of the target of an image orthicon camera tube by the scanning beam. Conclusions have been drawn relating to the exposure time of the tube and the way in which this influences the portrayal of a moving object. The tube used in these investigations was the 4½ in image orthicon type P.822 manufactured by the English Electric Valve Co. Ltd.

### **1. INTRODUCTION**

The resolution of a television camera depends partly on the optical system and partly on certain parameters associated with the camera tube. If the tube is an image orthicon, the most important of these parameters are the electric and magnetic fields in the image section, the spacing between the target and its mesh, lateral conduction of charge in the target and the effective thickness of the scanning beam at the target. Under normal operating conditions, a major cause of imperfect vertical resolution is the discharge by the beam during one field scan of some of that area of the target which constitutes the interlaced field.

The portrayal of moving objects depends mainly on the completeness of discharge of the target during each scan. If the discharge is incomplete, each field of the output signal contains contributions from information stored in the target during previous fields and the displayed output picture is degraded, in that each moving object in the scene is portrayed as a series of multiple images. If, on the other hand, the scanning spot is so large that it removes, during each scan, the majority of the charge which is in the province of the interlaced field, the storage time of the tube is a field period, rather than a picture period as it would be with a perfect scanning system.

### **2. THE PROCESSES OF CHARGING AND DISCHARGING THE TARGET**

The operation of the image orthicon camera tube was described briefly in earlier papers.<sup>1,2</sup> In this report, the discharge of the target by the scanning

beam is dealt with in greater detail because a more precise knowledge of the target charging and discharging processes is required if reliable conclusions are to be reached from the results of measurements on the performance of the tube. The main factor that was not taken into account previously is the effect of the initial target voltage on the efficiency of discharge of the target by the beam. The effects of lateral electro-static coupling between elements of the target were considered previously;<sup>2</sup> they are considered here in greater detail and from a slightly different viewpoint.

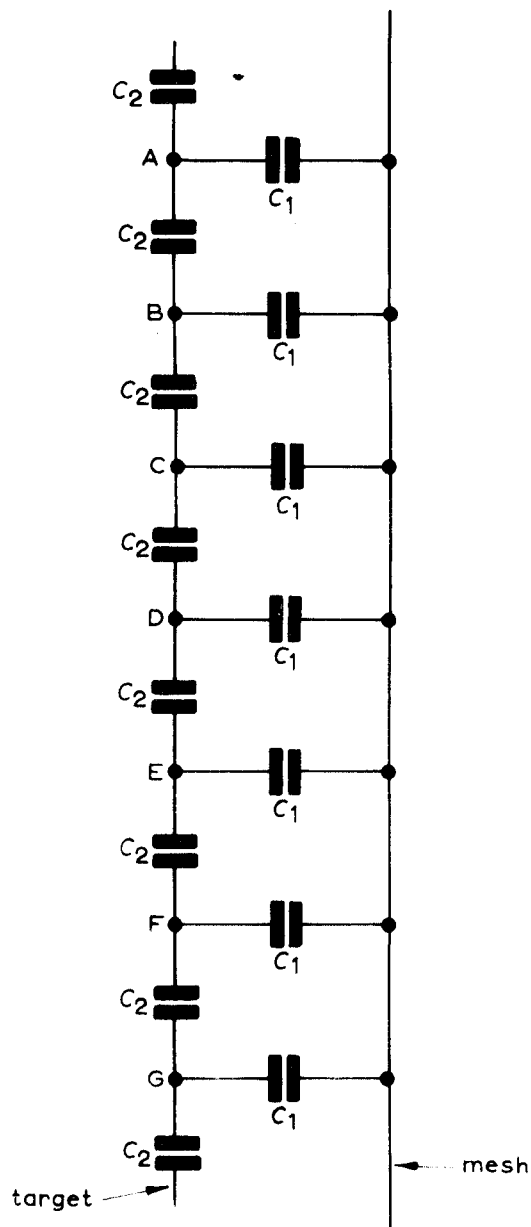


Fig. 1 - The representation of the target capacitance in terms of inter-element and element-to-mesh capacitances

## 2.1. The Process of Charging the Target

When an image orthicon tube is exposed to a scene consisting of a patch of high uniform brightness surrounded by an area of low uniform brightness, a corresponding charge pattern is built up on the target. If the brightness of the highlight is below the knee of the transfer characteristic, it produces, at the target, a patch of charge whose density is approximately uniform, but if the highlight brightness is above the knee of the characteristic, the potential of the corresponding target area is approximately uniform and is slightly more positive than that of the mesh. Only a few of the secondary electrons emitted from the area then arrive at the mesh, the remainder falling back on to the target.

The potential of an element of the target depends not only upon the charge on that element, but also upon charges on adjacent elements; for a given potential, the elements near the edge of a charged patch carry greater charge than those at the centre of the patch, the latter being surrounded by elements carrying similar charges.

The target may be considered as a large number of elements, each having direct capacitance  $C_1$  to the target mesh and lateral capacitance  $C_2$  to each of its neighbours;<sup>2,3</sup> this is illustrated in Fig. 1, which represents the capacitances associated with a vertical column of target elements, A, B, C, D, E, etc. If a



quantity of positive charge,  $+q$ , were placed on one of these elements (for example, D) it could be considered to be shared between the direct capacitance to the target mesh  $C_1$  and the capacitances to each adjacent element in all directions on the target surface, represented by  $C_2$ . The changes caused by the latter induce potentials at neighbouring elements C, E, etc. and thence, through further lateral capacitances, to more remote elements. Let  $C'$  denote the total effective capacitance of the element D, so that if the potential of D relative to the mesh is  $V$  then  $q = VC'$ . The ratio  $C'/C_1$  depends on the relative proportion of the target-to-mesh spacing to the dimensions of the target element, some numerical data being given in the Appendices.

When it is necessary to make a distinction between them  $C'$  will be called the 'small area' capacitance of the element and  $C_1$  will be called the 'guard-ring' capacitance, from the classical method of avoiding the effects of additional capacitances represented by  $C_2$  when measuring direct capacitances.

If equal quantities of charge,  $+q$ , were placed on two adjacent elements of the target, say, C and D, they would be raised to a potential  $V'$  which is greater than  $V$ . This can be considered in two ways, either by saying that because there is no potential difference across the capacitance joining C and D there is no charge on this capacitance and therefore the two applied charges are each shared between less capacitance than before, or alternatively, by saying that the potential at C due to both charges is the sum of the potentials that each would produce by itself, so the potential at C is raised above that due to the charge at C by an amount equal to the potential produced at C by a single charge  $+q$  at D. These ideas can be extended to show that:

- (i) If a charge  $+q$  is applied to each of the elements of a patch of the target the potential at the elements near the centre of the patch is higher than the potential at the edge of the patch.
- (ii) If all the elements in a patch of the target are raised to the same potential, the charges on the elements at the edge of the patch are greater than the charges on the elements at the centre of the patch.
- (iii) The potential is raised at points outside the charged area.

Fig. 2 illustrates these charge and potential distributions, but the shapes

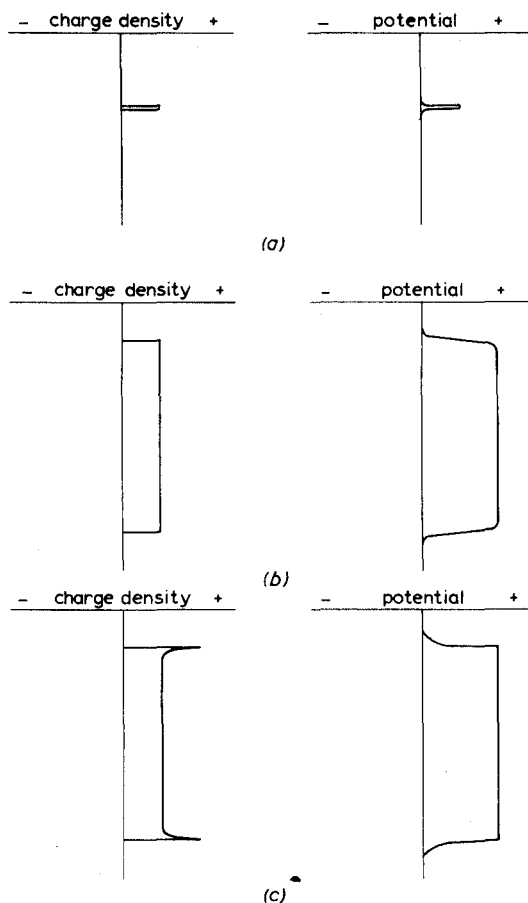


Fig. 2 - Distribution of charge and potential on the target

- (a) Distribution due to charge on a single element
- (b) Distribution due to charge of uniform density
- (c) Distribution of charge which produces a uniform potential over the charged area

of the curves are in many ways diagrammatic - the exact shapes depend on the permittivity of the target material and the ratio of the target thickness to the target-to-mesh spacing.

The target of an image orthicon camera is continuous, and the concept of isolated elements is artificial when applied to this tube. The electrostatic field of a continuous distribution of charge on the target can be deduced from first principles by considering the charge on an elementary area of the target and then integrating in order to find the effect of the whole charged area. Many of the results used in this report are qualitative and may be deduced from an elementary theory of electrostatics, but when quantitative results are required, it may be found that the best way of finding the effects of the charge induced into the target mesh is to find the effects of an image of the target charge, i.e., a charge distribution identical to that on the target but of opposite polarity. Its position is imagined to be as far behind the mesh as the target is in front of it, the mesh having been removed.

When a sharply defined area of the target is raised to a uniform potential, the electrostatic field produced is the same as that of a parallel-plate capacitor that has one plate larger than the other and has a thin layer of dielectric material, the glass of the target, just outside the gap between the plates. The field that would be produced without the layer of dielectric material, which will not differ significantly from the field with it, is shown in Fig. 3; the effects of the charged

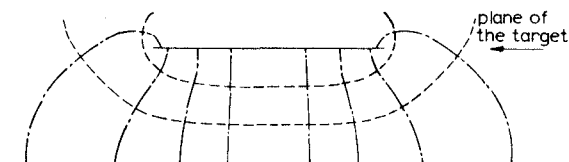


Fig. 3 - The electrostatic field between parallel electrodes

— Electrodes  
 --- Lines of force  
 ..... Equipotentials

area on the potentials at points of the target outside that area can be seen from the intersections of the equipotential lines with the plane of the target. The density of charge on the target is not uniform; for a very thin layer of charge the density at a point is directly proportional to the potential gradient measured at that point.

In practice, there will not be any sharp discontinuities in the charge and potential distributions as they will be smoothed out by such effects as aberrations in the optical and electron-optical systems and lateral leakage in the target. Also, this account of the process of charging the target implies, so far, that all the secondary electrons which leave the target are either collected by the target mesh or return to the points on the target from which they were emitted. Some secondaries emitted from one point return to a different point of the target; this slightly modifies the charge and potential distributions and causes the familiar black halo round very bright parts of the picture.<sup>4</sup> The effects of charge redistribution are not important in relation to the main subject of this report and further consideration of it will be left until later.

## 2.2. The Process of Discharging the Target

Meltzer and Holmes<sup>5</sup> have considered the collection of low-velocity scanning beam electrons by a conductive target in terms of the target potential and the

characteristics of the beam. They showed that a graph of target current plotted against the potential difference between the target and the cathode, Fig. 4, is exponential at low currents and linear over the middle range in the manner typical of thermionic diodes; it flattens off again at higher voltages because secondary electrons emitted from the target are collected by more positive electrodes in the tube. The initial (exponential) part of the curve shows that some beam electrons have higher emission velocities than others. By analogy with the random distribution of velocities of molecules in a gas, Meltzer and Holmes translated the distribution of beam-electron velocities into an equivalent 'beam temperature'. When the grid of the camera tube is made sufficiently negative to reduce the beam current nearly to zero, the beam temperature falls to a value close to the cathode surface temperature. Because the target of a camera tube has low conductivity the potential and current collection must be considered for each element of the target.

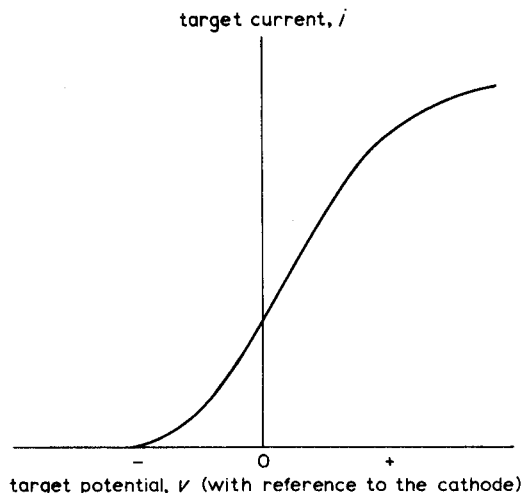


Fig. 4 - A typical target-current/  
target-to-cathode voltage  
characteristic

The quantity of charge deposited by the beam on an element of the target depends on both the rate at which electrons are collected and the time for which the beam rests on the element. Let  $C'$  be the small-area capacitance of an element of the target and let  $T'$  be the time for which the beam rests on the element, the diameter of the beam being greater than that of the element. If the beam is assumed to be of uniform density, we may relate the voltage of the element,  $v$ , and the current discharging the element,  $i(v)$  by the equation:

$$\frac{dv}{dt} = \frac{-i(v)}{C'}$$

Separating the variables and integrating,

$$\begin{aligned} \int_{v_2}^{v_1} \frac{dv}{i(v)} &= \int_0^{T'} \frac{dt}{C'} \\ &= \frac{T'}{C'} \end{aligned}$$

where  $V_1$  and  $V_2$  are the potentials of the element immediately before and immediately after it is scanned by the beam. If various simplifying assumptions are made  $T'/C'$  is the reciprocal of the rate at which the target is scanned, measured in  $\mu s$  per  $\mu F$ . Meltzer and Holmes assumed that this is equal to the ratio  $T/C$  where  $T$  is the total active scanning time and  $C$  is the total capacitance of the scanned area of the target. This is not strictly accurate, however, since  $C$  is a large-area capacitance while  $C'$  is a small area capacitance; the error is, in effect, only the use of a wrong scale factor and has no bearing on the qualitative results.  $T$  and  $C$  will, therefore, be used in the following analysis.

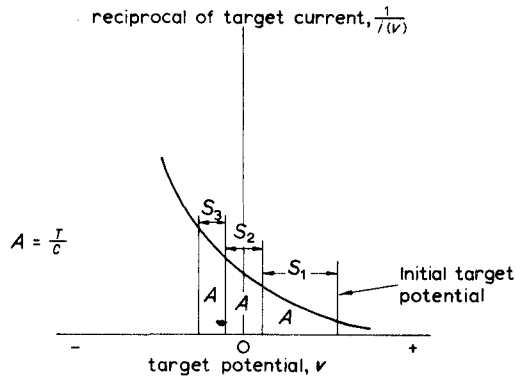


Fig. 5 - The reciprocal of target current plotted against target potential

that outputs  $S_1, S_2, S_3$ , etc. on successive scans can be derived from the curve by marking off areas  $A$ , equal to  $T/C$ , starting from the initial target voltage.

### 2.2.1. The Effect of the Initial Potential of the Target on Discharge Efficiency

The beam-acceptance curve will be treated as exponential for low values of  $v$  and linear for higher values, and relationships between  $S_1$  and  $S_2$  found for both cases. The exponential part of the characteristic may be written in the form:

$$i = ae^{kv} \quad (1)$$

where  $a$  is the value of  $i$  when  $v$  is zero and  $k$  is a positive constant which is inversely proportional to the beam temperature measured on the absolute scale.

If  $V_1, V_2, V_3$  are the voltages just before the 1st, 2nd and 3rd scans, then:

$$S_1 = V_1 - V_2 \quad (2)$$

and

$$S_2 = V_2 - V_3 \quad (3)$$

are proportional to the output signals on the first and second scans.

Thus we have:

$$A = \int_{V_2}^{V_1} \frac{dv}{i(v)} = \frac{1}{a} \int_{V_2}^{V_1} e^{-kv} dv \quad (4)$$

Putting  $c = Aak$ , this gives:

$$c = e^{-kV_2} - e^{-kV_1} \quad (5)$$

Re-plotting the 'beam-acceptance' curve of Fig. 4 as  $1/i(v)$  against  $v$ , (Fig. 5), the area under the curve between  $v = V_1$  and  $v = V_2$  is equal to  $T/C$ . The output signal is proportional to the charge absorbed from the beam, which is proportional to  $(V_1 - V_2)$ , the change of potential of the target element. Let  $S$  represent this change of potential.

If a bright part of the scene is extinguished (or moves to a remote part of the picture) successive scans will reduce the target potential. Since  $T$  and  $C$  may be assumed to be constant, each scan produces a change in  $v$  corresponding to an area under the curve equal to  $T/C$ , so

Multiplying both sides by  $e^{kV_1}$  gives:

$$e^{kS_1} = 1 + ce^{kV_1} \quad (6)$$

Alternatively, multiplying by  $e^{kV_2}$  gives:

$$e^{-kS_1} = 1 - ce^{kV_2} \quad (7)$$

Similarly, for the second scan:

$$e^{kS_2} = 1 + ce^{kV_2} \quad (8)$$

Adding equations (7) and (8):

$$e^{kS_2} = 2 - e^{-kS_1} \quad (9)$$

which gives a simple relationship between  $S_1$  and  $S_2$ .

Alternatively, taking logarithms of both sides of equations (7) and (8) and dividing gives:

$$\frac{S_2}{S_1} = - \frac{\log (1 + ce^{kV_2})}{\log (1 - ce^{kV_2})} \quad (10)$$

Putting:

$$x = ce^{kV_2} \quad (11)$$

then

$$\begin{aligned} \frac{1}{x} &= \frac{1}{c} e^{-kV_2} \\ &= \frac{1}{c} (c + e^{-kV_1}) \quad (\text{From equation 5}) \\ &= 1 + \frac{1}{c} e^{-kV_1} \\ &= 1 + \frac{1}{Aake^{kV_1}} \end{aligned} \quad (12)$$

Since  $A$ ,  $a$  and  $k$  are positive, it is clear that  $x$  is positive and less than 1.

$$\text{The ratio } \frac{S_2}{S_1}, \text{ which may be written as } - \frac{\log (1 + x)}{\log (1 - x)}, \text{ falls} \quad (13)$$

smoothly from 1 to 0 as  $x$  rises from 0 to 1.

Therefore, an increase in the value of  $V_1$ , which increases the value of  $x$ , reduces the ratio  $S_2/S_1$ .

The linear part of the beam acceptance curve may be expressed in the form:

$$i(v) = b + gv \quad (14)$$

where  $b$  and  $g$  are constants for a given total cathode current, both increasing as the current increases.

For the first scan of the target we have:

$$A = \int_{V_2}^{V_1} \frac{dv}{i(v)} = \frac{1}{g} \log \frac{b + gV_1}{b + gV_2} \quad (15)$$

$$\text{therefore} \quad b + gV_1 = e^{gA} (b + gV_2) \quad (16)$$

$$= e^{gA} (b + gV_1 - gS_1)$$

$$\text{therefore} \quad gS_1 = (b + gV_1) (1 - e^{-gA}) \quad (17)$$

$$S_1 = (V_1 + b/g) (1 - e^{-gA}) \quad (18)$$

Similarly:

$$gS_2 = (b + gV_2) (1 - e^{-gA}) \quad (19)$$

From this and equation (16) we get:

$$gS_2 = e^{-gA} (b + gV_1) (1 - e^{-gA}) \quad (20)$$

$$\text{But} \quad gS_1 = (b + gV_1) (1 - e^{-gA}) \quad (17)$$

$$\text{therefore} \quad S_2/S_1 = e^{-gA} \quad (21)$$

This shows that if  $V_1$  is sufficiently high for both  $V_1$  and  $V_3$  to be on the linear part of the beam acceptance curve, the ratio  $S_2 : S_1$  is independent of  $V_1$ .

Over the transition range, where  $V_1$  is on the linear part and  $V_3$  on the exponential part of the characteristic, there will be some decrease in the ratio  $S_2/S_1$  as  $V_1$  is raised.

If the beam-acceptance curve were precisely of the form  $i = ae^{kv}$  and if the target insulation were perfect, it would be possible to drive the target to any specified negative potential if it were scanned sufficiently often. In practice, neither of these conditions holds; usually two scans are sufficient to reduce the target potential to such an extent that the outputs on all later scans are below the level of the noise in the tube output and the target potential is stabilized at a level slightly negative with respect to the cathode. The scans producing the outputs  $S_1$  and  $S_2$ , therefore, virtually discharge the target and the result obtained earlier, that the ratio  $S_2 : S_1$  decreases as  $V_1$  increases, means that the efficiency of target discharge by the first scan increases as the initial target voltage is increased.

### 2.2.2. The Effects of a Change in Beam Current on Discharge Efficiency

The effects of reducing the beam current are shown in Figs. 6(a) and 6(b) (corresponding to Figs. 4 and 5 respectively). If the value of  $k$  in the formula  $i = ae^{kv}$  were constant, the ordinates of the two curves of Fig. 6(a) would be in a constant proportion for all values of  $v$ , and the two curves of Fig. 6(b) would be in the inverse proportion. Meltzer and Holmes found, however, that as the beam current is reduced, the beam temperature falls and  $k$  rises. As a result, the ratio of the ordinates of curve (ii) i.e. with reduced current, to those of curve (i) i.e. with normal current, in Fig. 6(a) increases steadily as  $v$  varies from the maximum negative value through zero to the maximum positive value corresponding to the exponential part of the curve. Conversely, in Fig. 6(b), which shows the reciprocal of target current plotted against target voltage, the ratio of the ordinates of curve (ii) to those of curve (i) fall steadily as  $v$  increases.

In Fig. 6(b),  $V_1$  represents the initial target voltage and the two shaded areas are equal, each being  $A = T/C$ , so that  $S_1$  and  $S_1'$  represent the output signals at the first scan of the target with normal and reduced beam current respectively. Clearly  $S_1$  is greater than  $S_1'$ .

The variation of the ratio  $S_2/S_1$  with beam current will be considered first for the linear part of the beam acceptance curve and then for the lower (exponential) part.

For the linear part of the relationship:

$$S_2/S_1 = e^{-gA} \quad (21)$$

shows that the ratio falls as  $g$  rises, i.e., as the beam current rises.

For the exponential part of the curve, the ratio is given by:

$$\frac{S_2}{S_1} = \frac{-\log(1+x)}{\log(1-x)} \quad (13)$$

where

$$\frac{1}{x} = 1 + \frac{1}{Aake^{kv_1}} \quad (12)$$

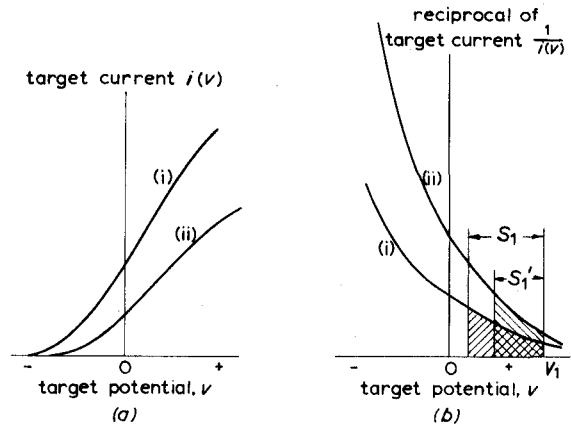


Fig. 6 - The effect of reducing the beam current

(a) On the beam-acceptance curve

(b) On the reciprocal of the beam-acceptance curve

(i) Normal current (ii) Reduced current

If the beam current rises the value of  $a$  rises but  $k$  falls, though less rapidly, so the behaviour of the product  $ake^{kV_1}$  depends on the relative importance of the three factors. If  $V_1$  is very small, or zero, the third factor is very closely unity and  $ake^{kV_1}$  varies in the same manner as  $ak$ , i.e. it rises as the beam current rises. If  $V_1$  is not small the third factor is dominant over practical ranges of  $a$  and  $k$ , so that for negative values of  $V_1$  a rise in current will again raise  $x$ , causing a fall in the ratio  $S_2/S_1$ . If  $V_1$  is appreciably positive the operating point moves from the exponential to the linear portion of the characteristic and equation (12) no longer applies.

Summarizing these results, it can be shown that if  $V_1$  is within the lower (exponential) or central (linear) part of the beam acceptance curve, an increase in beam current reduces the ratio of scan 2 output to scan 1 output.

### 2.2.3. The Influence of the Focus and Deflection Systems on Target Discharge

Using the ideas outlined in the previous sections, we may now consider the effect of the scanning process on the discharge of the target, making the assumption that, because the target is very thin, the potential difference between its faces is much less than the changes of potential difference between the target and its associated target mesh.

If there were no illumination of the photo-cathode and if the conditions inside the tube were ideal (in particular, if all electrons were to leave the cathode of the electron gun with velocities that lay within fixed limits and were to emerge from the final aperture of the gun correctly aligned with the magnetic field, and if the scanning conditions were ideal) the scanned area of the target would eventually be brought to a uniform potential such that the fastest electrons from the gun would just fail to land. Because of errors in alignment of the electron beam with the magnetic focusing field, and, to a lesser extent, because of the curvature of this magnetic field which is inherent in the scanning process, the electrons do not follow the lines of magnetic field precisely but travel in complicated paths similar in shape to a helical spring of varying pitch which has been bent near its centre in such a manner that the axis of the helix at one end of the spring is still parallel to the axis at the other end of the spring. Electrons that just reach the target do not have zero energy when they strike it, but have amounts of energy corresponding to their lateral velocities, and the initial potentials of the points on the target that they reach must correspond to these amounts of energy;<sup>6</sup> the difference between the kinetic energy of an electron when emitted from the cathode and the kinetic energy when it reaches the target is equal to the charge on the electron multiplied by the potential difference between the emission and collection points. As a result, the potential to which the target can be discharged varies over the scanned area in accordance with the variations in the angle of arrival of the electrons at the target during the scanning cycle, so that there would be a variation of output signal even if the initial potential of all points of the target, immediately before scanning, had been the same.

The electrons that strike the target with appreciable longitudinal velocity release a few secondary electrons.<sup>4,7</sup> The secondary emission ratio is small and depends to a small extent on the angle at which the electrons strike the target. Similarly, because of their helical motion, some of the electrons returning to the



first dynode strike it obliquely, but the angles their paths make with the normal to the dynode are always fairly small because the longitudinal components of velocity are high, corresponding to approximately 300 eV of energy.

These effects of imperfections in scanning are ignored in the following analysis unless they are specifically mentioned. Let us now consider the process of scanning the charge and potential distribution shown in Fig. 2(c), assuming that the illumination is present for an interval, less than one field period in duration, which does not include the period during which the charged area is scanned.

#### 2.2.4. Discharge of the Target when the Width of a Scanned Line is Equal to the Spacing of Lines in a Field.

Let Fig. 2(c) be taken as representing the charge-density and potential distributions along a section of the target in the field direction. When the beam scans the area of the target immediately above the charge it finds a small positive potential, so it deposits a small negative charge. This slightly reduces the voltage at the top of the positively charged area as shown diagrammatically in Fig. 7(a). Nevertheless, when the beam first crosses the fully charged area, it finds the target at a high potential. The discharge efficiency is high ( $V_2/V_1$  small) and the charge deposited is equal to the product of  $(V_1 - V_2)$  and the small-area capacitance  $C'$ . Fig. 7(b) shows the total quantity of negative charge added to the target during this and the preceding lines and the resulting potential distribution. The area scanned by the first line to cross the fully charged region of the target carried, immediately before scanning, a quantity  $V_1 C''$  of positive charge, where  $C''$  has a value that lies between the small-area capacitance  $C'$  and the guard-ring capacitance  $C$  and that depends on the influence of the remainder of the positive charge on the target. Thus, even though  $V_2$  is not zero, the value of  $(V_1 - V_2) C'$  may be similar to, perhaps even greater than, the value of  $V_1 C''$ , which means that the quantity of negative charge deposited on an area in one line of scan can exceed the positive charge existing on the corresponding area on the image side of the target.

When the next line is scanned, the beam finds a slightly lower value of  $V_1$ , because the unscanned area of positive charge has been reduced while the field due to the area already scanned is weak and may even be negative, but this difference in  $V_1$  is too small to be shown in Fig. 7.

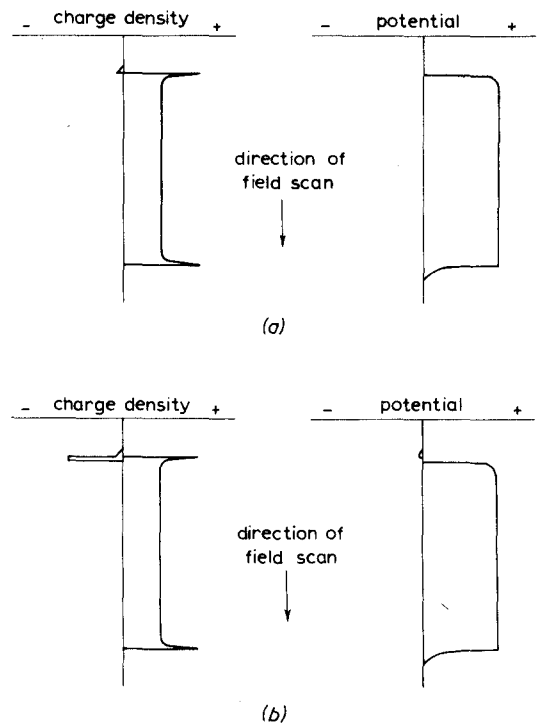


Fig. 7 - The start of the scanning of the charged area by a 'wide' beam (illumination above the knee of the transfer characteristic)

- (a) Distribution just before the scan reaches the charged area
- (b) Charge and potential distributions immediately after scanning along the first line that passes through the charged area

Let us assume that the charged area is symmetrical about an axis parallel to the line-scan direction. The potential at a point on this axis may be considered as having two equal components, one due to each half of the charged area. If one half of the area is scanned, the negative charge deposited by the beam is approximately equal to the original positive charge on the scanned area. One half of the total positive charge has, in effect, been removed so the potential at the point on the axis of symmetry is halved. The following line of the scan does not lie along this axis of symmetry but lies in the area not previously scanned, so the value of  $V_1$  is not reduced by as much as one half of the potential existing before the scan started.

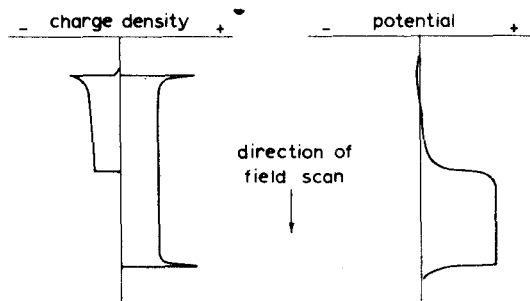


Fig. 8 - Distribution of charge and potential half way through scan 1

Even so, there is a significant reduction in  $V_1$  and with it a reduction in the negative charge deposited and, therefore, in the output signal. The distributions of charge and potential are then somewhat as shown in Fig. 8. (Once again, it is emphasized that these diagrams are not to scale.)

As the field scan continues, the beam is brought into the area where the positive charge is increasing, so the ratio of decrease of  $V_1$  with field scan is less: hence the negative charge deposited by each line, and therefore the output signal, falls off less rapidly. The variation of output signal, line-by-line, during the first scan follows the shape of the negative charge curve of Fig. 9(a).

In the experiments to be described in Section 5, the illumination of the photo-cathode was switched off just before the scanning of the charged area and was not switched on again until several field scan cycles had been completed. In the interval between the first and second scans of the charged area, there is a flow of charge through the target. If the target is thin enough, and its conductivity high enough, the resulting charge and potential distributions are as shown in Figs. 9(b) and 9(c). The second scan then encounters a charged area whose potential

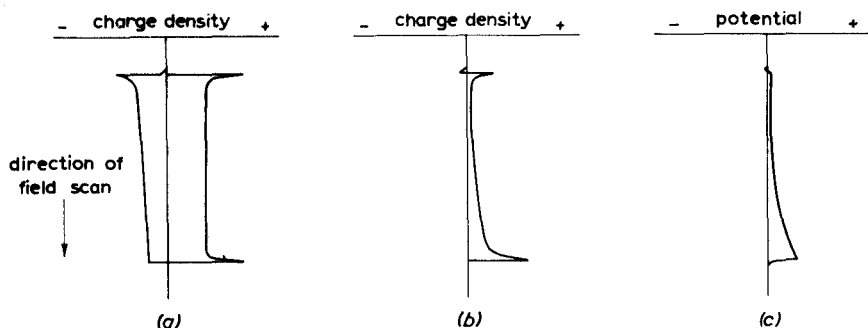


Fig. 9 - Distribution of charge and potential at the end of scan 1 and start of scan 2

- (a) Charge distribution at end of scan 1
- (b) Charge distribution at start of scan 2
- (c) Potential distribution at start of scan 2

increases line-by-line and the output on this scan also increases line-by-line, though this is less marked than the variation in the initial potential distribution, because of the effects already described. These results were confirmed by observations (see Section 5.1.).

There are corresponding variations in output signal as the beam scans a line across the charged area, the initial potential,  $V_1$ , being slightly lower at the end of the charged part of the line than at the beginning. The effect is less marked than it is in the field direction because the charge on the adjacent line has more influence on the potential at a point than the charge at a more distant point on the same line.

#### 2.2.5. Discharge of the Target when the Width of a Scanned Line is Equal to the Spacing of Lines in a Picture

If the scanning spot is assumed to discharge strips equal in width to one picture line (i.e., the spot diameter is one half of that considered in Section 2.2.4.), the effects are different. The potential at a target element that is about to be scanned is less affected by the scanning of previous lines of the field, because there is positive charge still left on the adjacent lines in the scanned area which belong to the interlaced field; this is discussed further in Appendix I. As a result, the shading effects are far less serious than those produced by the wider beam. In practice, the effective width of the beam lies between these two conditions, and may vary over the scanned area.

#### 2.2.6. The Differences Between the Effects of Intermittent and Continuous Illumination of the Photo-Cathode

The previous sections dealt with the output to be expected from an image orthicon camera tube when the illumination of the photo-cathode ceases before the corresponding charged area of the target is scanned. If the illumination is continuous, the results are modified, because photo-electrons reach the target continuously and the emission of secondary electrons from the image side of the target modifies the charge distribution over the charged area while the area is being scanned.

In Section 2.2.4., it was shown that there is a tendency for the potential at the bottom of a charged area to drop as the area is scanned. When the illumination is continuous, the rate of charge by secondary emission of this part of the charged area is slightly increased and this, to some extent, offsets the fall in potential due to the discharge of the remainder of the charged area.

When the tube is operating above the knee of its transfer characteristic, the charging of the target is limited by the potential to which it can rise. If the potential of the unscanned part of the charged area could be kept up to this limiting voltage by secondary emission, the output from all lines would be the same, but under practical conditions, the rate of charge of the target is too low to achieve this. It has been shown that Figs. 8 and 9 represent the conditions at the middle and the end of a scan that occurs after illumination has ceased. When the illumination is continuous, the density of charge deposited by the beam during the early part of the scan falls off in a similar way because the continuing secondary emission

has not sufficient time to have much influence, but the charge deposited on a later part of the scan is greater than for intermittent illumination. This is in agreement with the results of measurements described in two other reports in this series.<sup>2,8</sup>

### 3. DESCRIPTION OF THE APPARATUS

The camera channel used for the investigation was the camera tube test bench which has been described elsewhere.<sup>9</sup>

In the experiments, a special form of light source was required in order to produce a flash of light of variable duration at a repetition rate of one flash every 12 television fields; it was also necessary to produce a rectangular patch of light, in the object plane, which moved in a horizontal direction during the period of exposure. Suitable apparatus, shown diagrammatically in Fig. 10(a), was developed consisting of a fixed defining aperture together with a disk with a spiral aperture, see Fig. 10(b), mounted on a rotating shaft; the defining aperture was illuminated by means of the optical system shown. The duration of the interval during which the defining aperture was illuminated was controlled by a shutter disk, see Fig. 10(c), rotating behind a fixed metal sheet having a narrow slot cut in it.

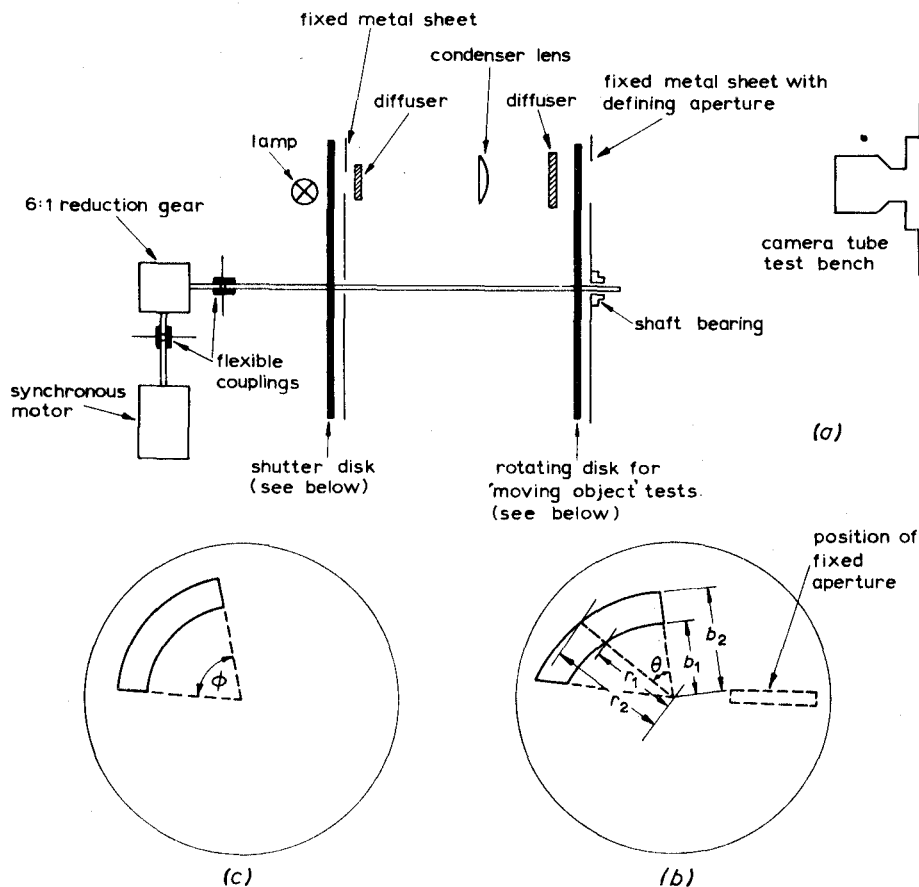


Fig. 10 - Mechanical details of the equipment

- (a) Schematic diagram of the equipment as seen from above
- (b) Disk used to represent a moving object
- (c) The shutter disk

The shaft was driven at 250 r.p.m. (i.e., one field period was equivalent to 1/12th rev.), so that the duration of camera-tube exposure could be altered by changing the length of aperture in the shutter disk. If the duration of the exposure required was, for example, 0.9 of a field period, then  $\phi$  was adjusted to be  $0.9 \times 360^\circ \div 12 = 27^\circ$ . The shaft was driven through a 6 : 1 reduction gear, by a synchronous motor running at 1,500 r.p.m. For measurements concerned with the portrayal of moving objects, the disk containing the spiral aperture was coupled to the rotating shaft; when a stationary bright patch was required, this disk was uncoupled from the shaft and held stationary.

The television waveform generator used in the experiments was supplied with a 50 c/s locking signal derived from the mains; this locking signal was adjustable in phase so that the mechanical shutter could be arranged to open at any required point in the television field.

#### 4. EXPERIMENTAL METHOD USED FOR INVESTIGATION OF TARGET DISCHARGE

The shutter was set to open for 0.9 of a field period and the relative timing of camera-tube exposure and scanning was adjusted so that the whole of the exposure occurred between successive scans of the relevant part of the target area. It was found that the relative timing of exposure and field scan could be accurately adjusted by observing the waveform of twelve output fields on an oscilloscope; the phase of the waveform generator locking signal was adjusted so that the output corresponding to the field scan immediately prior to the start of the illumination was just reduced to zero, so that the following field received the whole of the exposure between scans. The target was thus re-charged once every twelve fields, the charge and discharge occurring separately. The output obtained during the first scan immediately following exposure was termed the 'scan-1 output' and the output from the next (interlaced) scan was termed the 'scan-2 output'. Usually, these were the only two fields which gave measurable output, but under some conditions, outputs were measured during scans 3, 4 and 5; measurable output obtained during scans other than the first two indicated that the beam was not discharging the target effectively. If the tube were to resolve fully the vertical information corresponding to the number of scanning lines per picture employed, and there was complete independence between the scanning of odd and even fields, the output during scans 1 and 2 would be equal. In practice, however, some of the information on adjacent lines is removed during the first scan. If the signal-current output on scan 1 is  $I_1$  and the signal-current output on scan 2 is  $I_2$ , the ratio  $I_2/I_1$  is an indication of the degree to which the tube performance falls short of ideal in this respect. Capacitive coupling\* between target elements and poor scanning-spot size result in the output during scan 2 being much less than that during scan 1, and serious failure to discharge the target is indicated by the presence of signal output during scans 3 and 4.

#### 5. EXPERIMENTAL RESULTS

##### 5.1. Factors Investigated in order to Ascertain Their Effects on the Discharge of the Target

Both the effectiveness of the scanning-spot in discharging the charge pattern built up on the target and the effective scanning-spot size are functions of tube design and operation.

\*See Appendix 1.

The main factors involved are as follows:

- (i) the basic setting-up of the tube, in particular the adjustment of alignment currents;
- (ii) beam-focus and target mesh potentials;
- (iii) beam current;
- (iv) target temperature;
- (v) illumination level;
- (vi) the form of the scanning raster (i.e., interlaced or non-interlaced);
- (vii) the velocity of the scanning spot in the 'line' direction;
- (viii) the spacing between adjacent scanning lines.

It was found that the majority of tube-operating conditions could be varied without affecting the ratio of the output during scan 1 to the output during scan 2. It was also found that when a patch of very positive charge was located near the bottom of the scanned target area, serious shading of the type described in Section 2.3.1. occurred. Much less shading was produced when the charge patch was located near the centre of the target and all the measurements to be described were made during a line occurring approximately in the centre of the field scan.

Those operating conditions that had a marked effect on the ratio  $I_2/I_1$ , as defined in Section 4, are considered individually in the following sections.

Varying the currents in the alignment coils was found to affect the ratio  $I_2/I_1$  appreciably; however, the effects of mis-alignment were not investigated quantitatively and all the following measurements were made with the tube aligned correctly.

## 5.2. The Effects of the Beam-Focus and Target Mesh Potentials on the Discharge of the Target

When the beam was accurately focused, it was found that the scan 1 signal was at minimum and the scan 2 signal at a maximum. This was to be expected since, during each field scan, the focused beam discharges a minimum area of the target. No numerical results are given because of the difficulty in stating precisely the amount of defocusing present at any time. There was, however, no consistently measurable difference in results between the two focus modes used (i.e. with the wall anode at either 150 V or at 210 V above cathode potential). No difference in the ratio  $I_2/I_1$  was observed with the target-mesh potential set at either + 2 V or + 3 V with respect to 'cut off', the cut-off potential being defined as the target-mesh potential necessary just to prevent the beam landing on the charged target. All measurements quoted were made with the wall anode at the 210 V focus and the target mesh at + 3 V above cut off.

### 5.3. The Effect of Beam Current on the Discharge of the Target

This investigation was carried out by measuring the outputs of successive scans at different beam currents. The tube was exposed to a point half a stop above the knee of the transfer characteristic, the 'knee' being defined as the illumination level at which the point-gamma equals 0.5; in this case the knee corresponded to a photo-cathode illumination of 0.065 ft-C (0.70 lux).

The results are shown in Fig. 11 in which the normalized output signal is plotted against the tube cathode current, the latter being a measure of the beam current, although not equal to it quantitatively.<sup>1</sup> It will be seen that, as the cathode current rises from a low value, the output during scan 1 rises, but the output during scan 2 falls. At higher values of cathode (beam) current the ratio of the outputs changes only slowly. In normal operation the minimum beam current necessary to discharge the target is used; greater beam current merely increases noise and shading, and degrades resolution. In these measurements, it was found that satisfactory operation was obtained by adjusting the current so that the scan 1 signal output was 5% less than the maximum obtainable. The output on scan 2 is then approximately 24% of the maximum output on scan 1. This is consistent with the ideas developed in Section 2.2. and in Appendix I.

The most interesting feature of the graphs shown in Fig. 11 is that when the cathode current was low, the second-scan output was approximately equal to the first-scan output. At very low currents the scan 2 output exceeded the scan 1 output, particularly at higher illuminations than that shown in Fig. 11, but the existence of any output on scan 1 indicates that the target had been partially discharged and that its potential was, therefore, reduced. The fact that the scan 2 output may exceed the scan 1 output implies that the conditions at the target, during scan 2, were more favourable for discharge. The results are consistent with there being some secondary

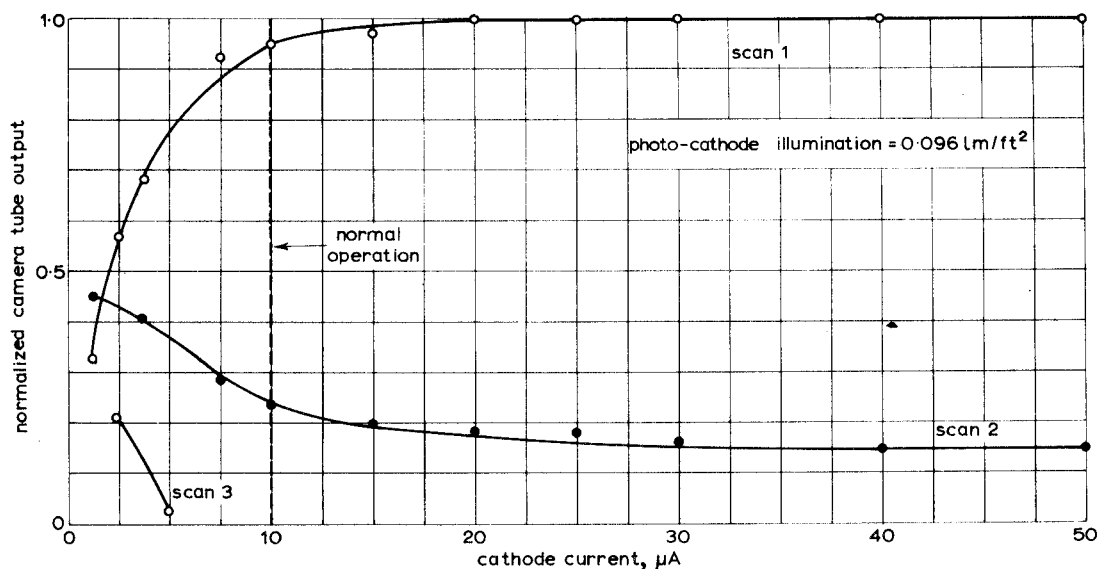


Fig. 11 - The effect of cathode current on target discharge

emission from the scanned side of the target, an effect which has been known for many years.<sup>4,7</sup> Two other effects of this secondary emission are, first, to reduce the depth of modulation of the return beam and, secondly, to lower resolution by increasing the effective cross-section of the scanning beam.

#### 5.4. The Effect of Target Temperature on the Discharge of the Target

A thermo-couple junction was attached to the tube envelope in the vicinity of the target in order to measure the external glass temperature and, although this did not measure the temperature of the target itself, it gave a useful indication under steady-state conditions. The scan 1 and scan 2 outputs were measured at several light levels as the tube temperature increased and the ratio  $I_2/I_1$  was plotted against temperature. The results are shown in Fig. 12. From the curves it will be seen that the ratio of the outputs during the first and second scans, at all exposures, became less as the tube warmed up. This indicates that, at normal operating temperature, the target resistance is such that significant charge leakage occurs between vertically adjacent picture elements in 1/50 second.

At low light levels (0.012 ft-C) (0.13 lux) the ratio  $I_2/I_1$  is high even at high temperatures. This is because the efficiency of discharge is low for low target potentials, so that only small potential gradients are produced on the target by the action of scanning. At high light levels (0.096 ft-C) (10.3 lux) the change of

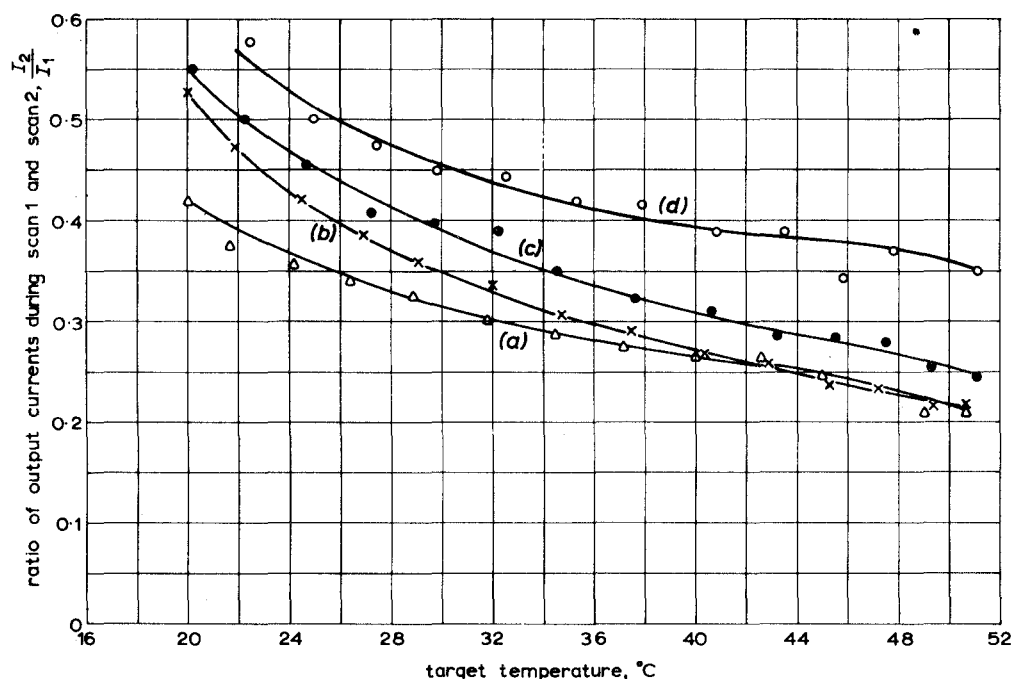


Fig. 12 - The effect of target temperature on target discharge

- (a) Photocathode illumination 0.096 lm/ft<sup>2</sup>
- (b) Photocathode illumination 0.047 lm/ft<sup>2</sup>
- (c) Photocathode illumination 0.025 lm/ft<sup>2</sup>
- (d) Photocathode illumination 0.012 lm/ft<sup>2</sup>



lateral leakage with temperature again appears to have a reduced effect upon the ratio  $I_2/I_1$ ; the lowest curve in Fig. 12 shows a consistently low ratio which does not vary greatly with temperature. The greatest dependence on temperature of the ratio  $I_2/I_1$  occurs at the intermediate light levels of about 0.074 ft-C (0.51 lux). At these levels the discharge efficiency is high producing the maximum potential gradient on the target after the first scan and hence the ratio  $I_2/I_1$  is more influenced by the amount of lateral leakage between successive scans. At higher brightness levels the charge on the target is denser, so that when the beam starts to discharge an element of the target a lateral electrostatic force is produced, which tends to spread the beam in a way that cannot be compensated by an adjustment of the beam focus control.

As a subsidiary experiment, the tube was continuously exposed to a vertical grating pattern corresponding to 2.4 Mc/s for 405-line scanning. The ratio of the magnitude of the signal corresponding to the grating to that of a large white area was measured at various temperatures, using a representative illumination level lying just below the point on the contrast-law characteristic at which the point-gamma equals 0.5. The contrast-law is shown in Fig. 13. The change of horizontal resolution with

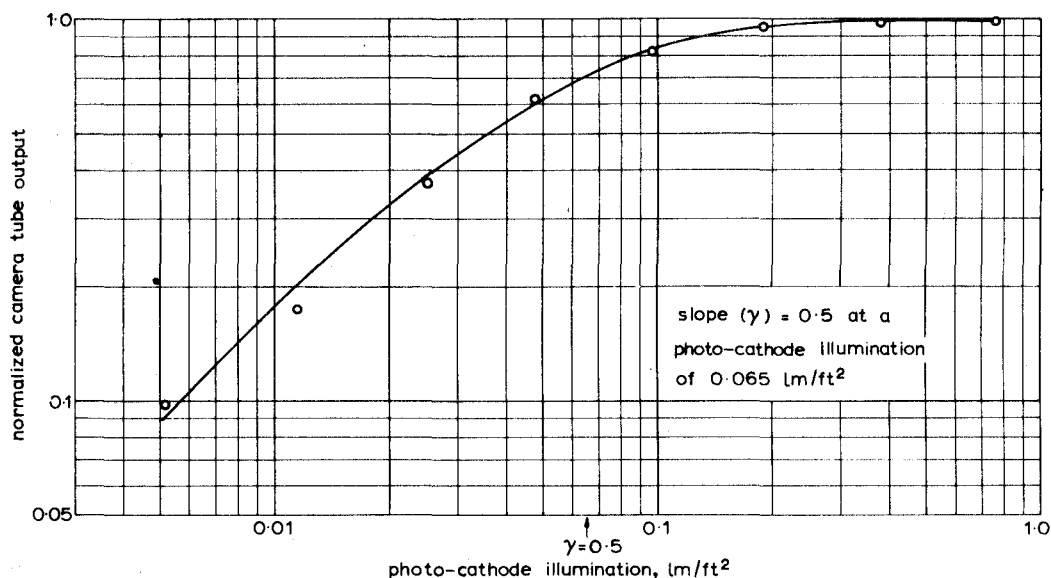


Fig. 13 - Contrast-law characteristic of camera tube

temperature is shown in Fig. 14, from which it will be seen that the resolution of the tube at 2.4 Mc/s (for 405-line scanning) is nearly 3 dB worse at 45°C (normal working temperature) than at 20°C.

In order to confirm that significant lateral leakage occurs between adjacent picture elements in 1/50 second, some alterations were made to the apparatus permitting the introduction of a delay of one, two, three or more whole fields between the exposure of the camera tube and the scanning of the information recorded on the target. Microswitches, operated by the rotating shaft, were used to generate a negative-going pulse that was added to the target blanking. The leading edge of the pulse coincided with the start of that field during which the defining aperture was illuminated, and the pulse duration was made equal to a whole number of field periods,

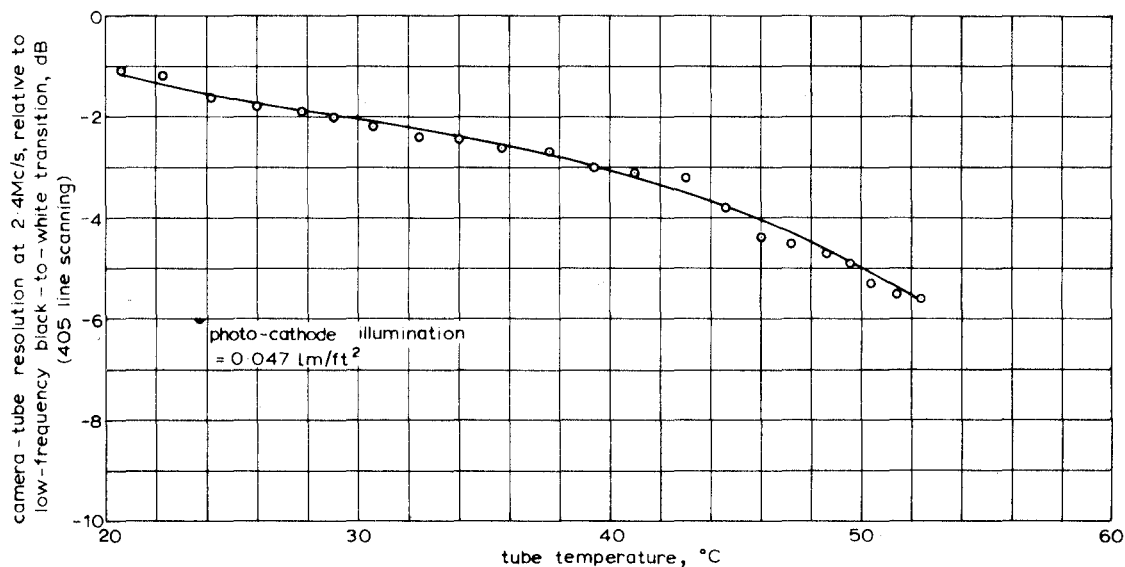


Fig. 14 - The effect of target temperature on the horizontal resolution of the camera tube when exposed continuously

so that the scanning of the target charge was delayed by this amount. A test was made in order to prove that the application of target blanking, during the illumination period, did not affect the charge stored on the target.

The 2.4 Mc/s grating was mounted, as before, over part of the defining aperture. Measurements were made of the ratio of 'grating' signal to 'white-bar' signal at an illumination level corresponding to normal white exposure of the bar ( $\frac{1}{2}$  stop above the  $\gamma$  equals 0.5 point of the contrast law) for delays of 1 and 3 field periods after an exposure lasting 0.9 fields. Figs. 15 and 16 show the result of these measurements. The two 'no-delay' curves should be identical, in fact at 50°C, there is a discrepancy between them of 1.4 dB. This is probably due to a slight maladjustment of beam focus when making measurements shown in the one-field delay curve (Fig. 15); at the temperature at which the focus was adjusted, a slight error was not easily detectable. The results obtained confirm that as the delay between exposure and scanning is increased from one field period to three field periods, at any particular temperature, there is an increased loss of resolution.

#### 5.5. The Effect of Illumination Level on the Discharge of the Target

The upper curve of Fig. 17 shows the ratio  $I_2/I_1$  as a function of illumination level. It will be seen that the ratio falls as the illumination is increased. This is caused by several effects, notably increased spot size due to the charge on the target producing lateral electrostatic fields at the point where the beam lands, and greater discharge efficiency on the first scan due to the higher target potential at high illuminations. In an attempt to separate the effects of changes in the discharge efficiency and effective spot size, the measurements described in the following section were made.

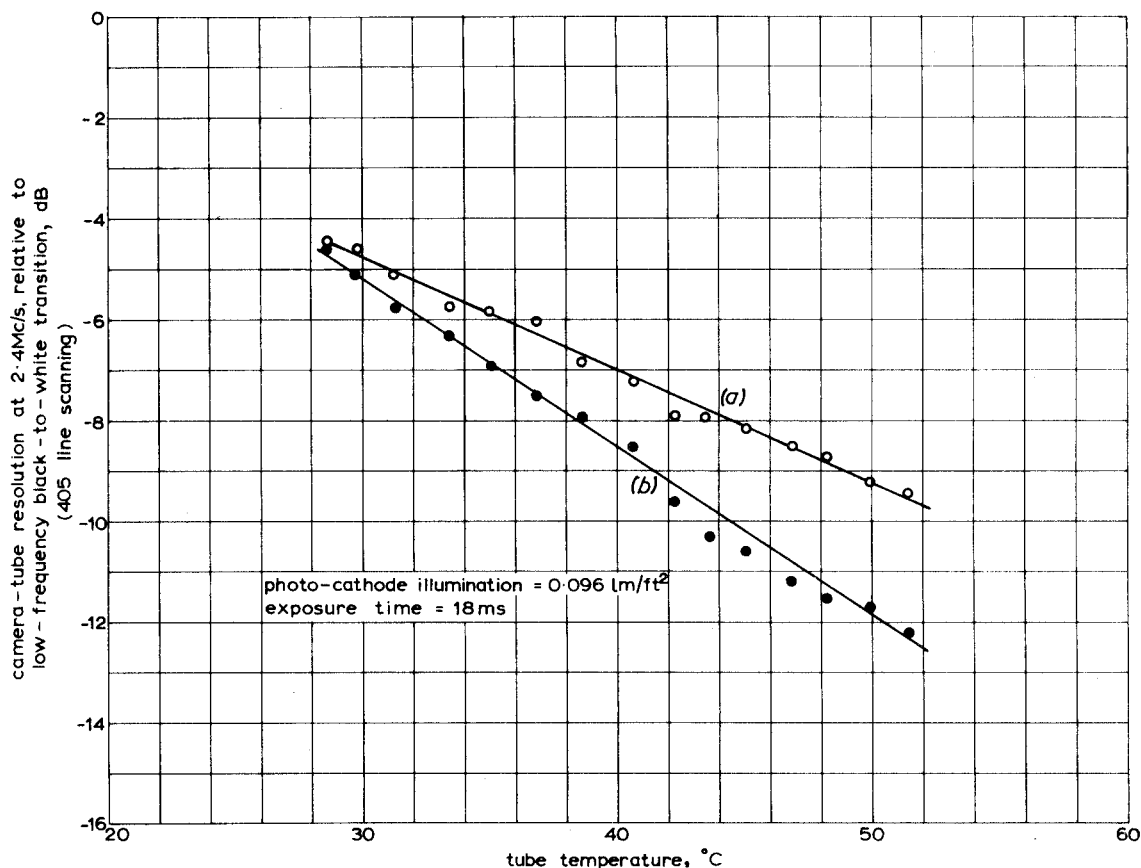


Fig. 15 - The effect of target temperature on the horizontal resolution of the camera tube when exposed intermittently

- (a) No delay between end of exposure and scanning
- (b) 20 ms delay between end of exposure and scanning

#### 5.6. The Efficiency of Target Discharge as a Function of the Type of Scanning Raster Used

The experiment described in the previous section was repeated using different numbers of scanning lines per field; in all cases there were 50 fields per second.

1. 202½ lines per field, successive fields interlaced, i.e., normal 405-line scanning.
2. 216 lines per field, successive fields superimposed, i.e., sequential scanning.
3. 312½ lines per field, successive fields interlaced, i.e., normal 625-line scanning.
4. 312 lines per field, successive fields superimposed, i.e., sequential scanning.

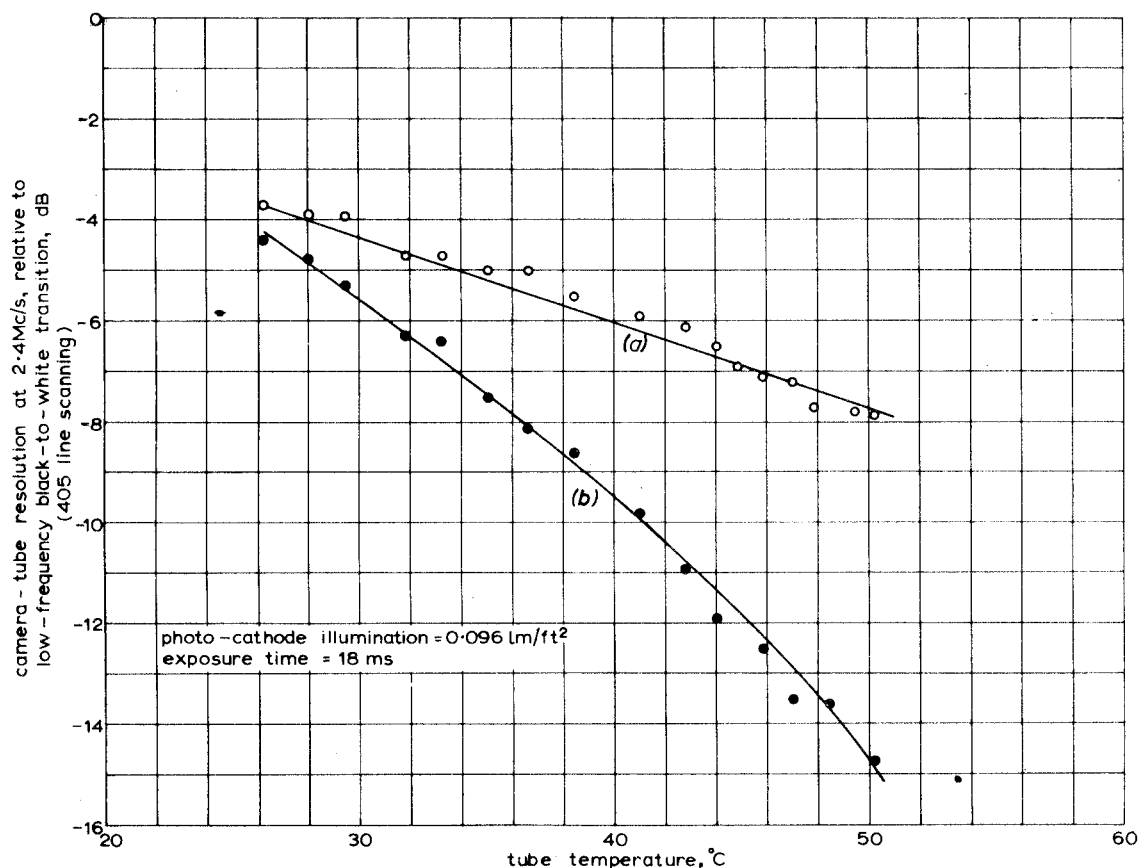


Fig. 16 - The effect of target temperature on the horizontal resolution of the camera tube when exposed intermittently

- (a) No delay between end of exposure and scanning
- (b) 60 ms delay between end of exposure and scanning

The results are shown in Fig. 17 and it will be seen that at all illumination levels, the ratio  $I_2/I_1$  obtained with 216-line sequential scanning was less than half that obtained with interlaced 202½-line scanning. This indicates that, on the one hand, approximately half the output observed on the second scan, when this is interlaced with the first, is attributable to target charge situated in areas between the lines of the first scan, and, on the other hand, half the output is due to incomplete erasure during the first scan. If the second-scan output, with interlaced scanning, had been entirely due to incomplete erasure during the first scan, no difference in the ratio would have been observed when using sequential scanning. If, however, the second-scan output, when using sequential scanning, had been entirely due to target charge in areas situated between lines of the first scan, the output on the second scan would have been zero.

Some confirmation of this is provided by the results obtained using an increased number of scanning lines. It will be seen that, except at low levels of illumination, the use of either interlaced or sequential scanning with approximately

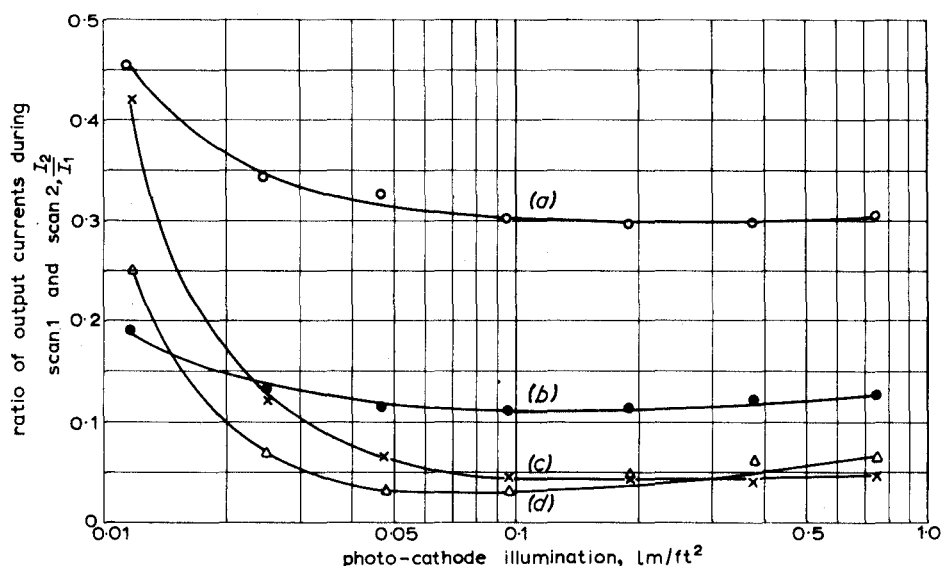


Fig. 17 - The effect of illumination on the discharge of the target, using interlaced and sequential scanning (10% overscan of target)

- (a) 405-line interlaced scanning
- (b) 216-line sequential scanning
- (c) 625-line interlaced scanning
- (d) 312-line sequential scanning

300 lines per field has little influence upon  $I_2/I_1$ ; this indicates that, under such circumstances, almost all the target charge located between the lines of the first scan is removed by the first scan.

It will also be noticed from these curves that, with approximately 300 lines per field, the effectiveness of erasure is greater than it is with some 200 lines per field, even when sequential scanning is employed. In the foregoing discussion of Fig. 17, a simplifying assumption was made in that no account was taken of lateral charge leakage at the target (see Section 5.4.). Some of the second-scan output obtained under sequential scanning conditions may, in fact, be due to leakage of charge from unscanned areas of the target situated between the lines of the scan into areas just discharged by the first scan; this leakage can take place throughout a full field period, thus adding to the charge remaining as a result of incomplete erasure during the first scan. This lateral leakage of charge, however, cannot occur if no unscanned areas exist between the lines of any one field; these conditions appear to apply, at high light levels, with 312-line sequential scanning, thus the second-scan output is less. Over the majority of the illumination range, the difference in the ratio  $I_2/I_1$  for 312-line and 216-line sequential scanning is approximately 2 : 1; this leads to the conclusion that, with the latter form of scanning, half the output during the second scan is due to incomplete erasure by the first scan, the other half being due to lateral leakage of target charge.

#### 5.7. The Effect of Line Scan Velocity on the Discharge of the Target

It was observed that, to some extent, the ratio  $I_2/I_1$  depended on the line scan velocity, which could be controlled by varying the amplitude of the line scan.

Measurements were made using both 405-line and 625-line scanning; in each case the scanning velocity was calculated by measuring the duration of the light pulse produced by the defining aperture (c.f. Fig. 10(a)). The results of the measurements using 405-line scanning are shown in Fig. 18 and the ratio  $I_2/I_1$ , for both 405-line and

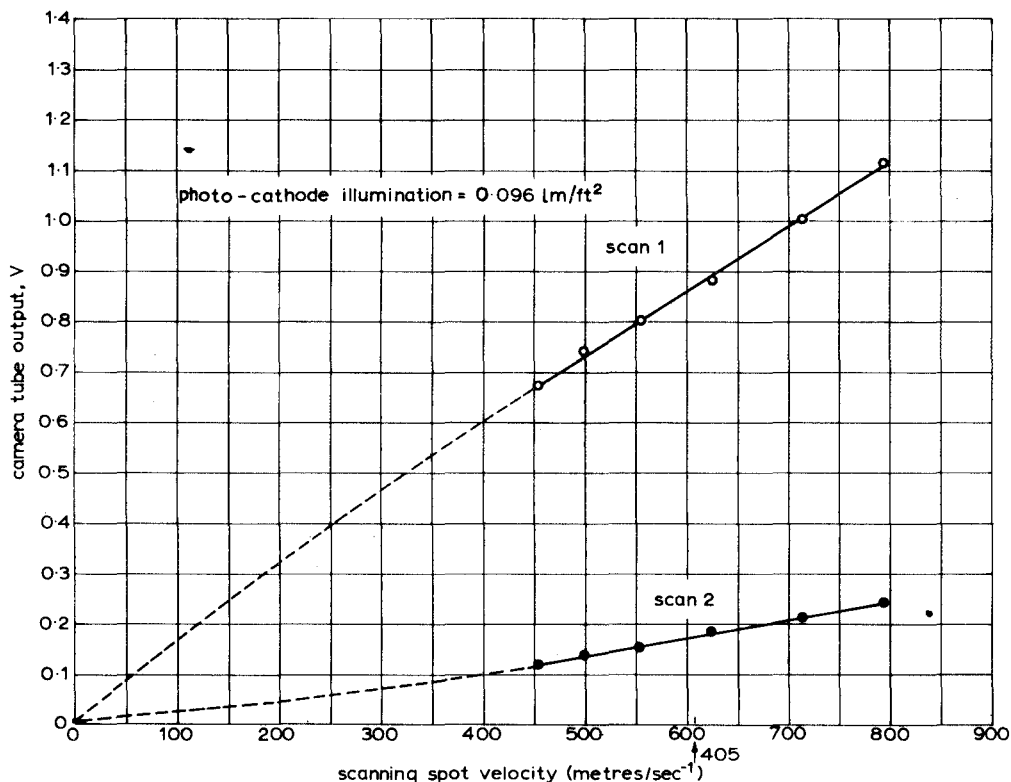


Fig. 18 - The effect of line scan velocity on the discharge of the target (405-line scanning)

The arrow shows the velocity corresponding to the normal 405-line standard

625-line scanning, is shown in Fig. 19. It will be seen, from Figs. 18 and 19, that, for 405-line scanning, the first and second-scan outputs are nearly proportional to the scan velocity; however, the ratio  $I_2/I_1$  does not remain exactly constant, but rises slightly with scanning velocity. In the case of the 625-line standard  $I_2$  is very small; although the results are probably not very reliable, the same rise in the ratio  $I_2/I_1$  is observable. In Fig. 18 the curves have been extrapolated towards the origin through which they must pass, since with no scanning velocity there can be no significant continuous output. It will be seen that the first-scan output curve is slightly convex upwards, while the second-scan output curve is slightly concave upward, these shapes accounting for the change in the ratio  $I_2/I_1$ . The results are consistent with a theory of target discharge given in Appendix 2.

#### 5.8. The Effect of Line Spacing on the Discharge of the Target

The effect of varying the line spacing was investigated, since this must have a direct bearing on the discharge mechanism of the target and it is also a factor

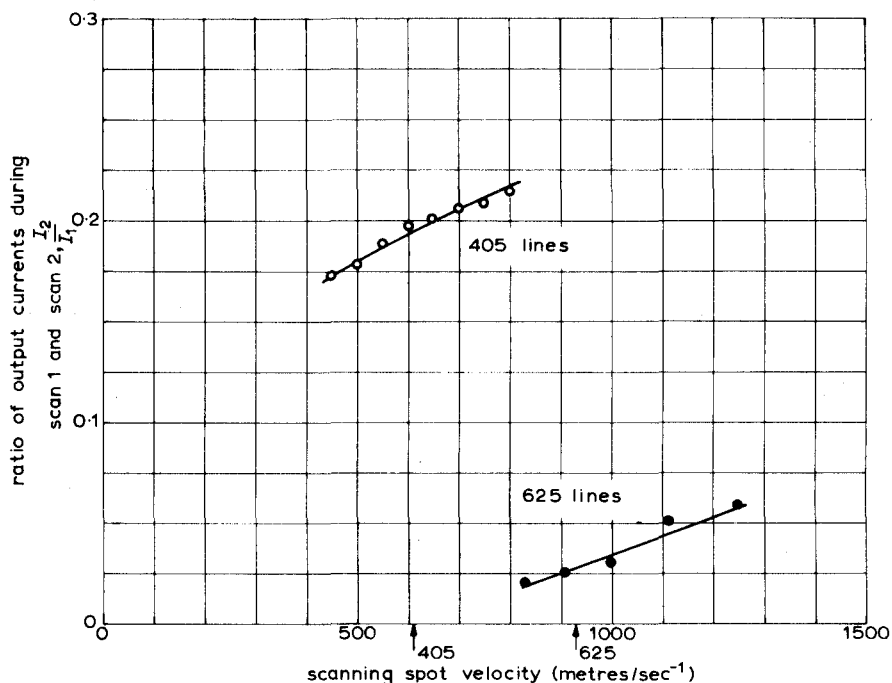


Fig. 19 - The effect of line scan velocity on the discharge of the target

The arrows show the velocities corresponding to the normal 405-line and 625-line standards

that changes significantly with a change of line standard. The change of spacing was achieved by varying the vertical-scan amplitude; this was monitored by measuring the voltage developed across a resistor permanently connected in series with the field-scan coils. A first series of measurements was made using the 405-line scanning standard and the scan amplitude was varied so as to explore a range of line spacings extending from 320 to 1800 active lines per picture height. In the measurements, first and second-scan outputs were measured at various line spacings and at three different levels of illumination.

A further series of measurements was made, using a 135-line scanning standard, in order to investigate the effect of very large line spacings. In this way, it was possible to reduce the effective number of scanning lines to be less than 120, but, unfortunately, this method of reduction reduces the line repetition frequency to 3.375 kc/s, which means that both the line-scan velocity and the line spacing have been changed; nevertheless, the way in which the ratio  $I_2/I_1$  changes remains of interest. The results of these measurements are shown in Figs. 20, 21 and 22.

From Fig. 20 it will be seen that the first-scan output increased almost linearly as the line spacing was increased, until a spacing equivalent to approximately 525 lines per picture height was reached. No second-scan output became apparent until a line spacing equivalent to 625 lines was reached, at which point the second-scan output increased nearly linearly with line spacing over the range examined.

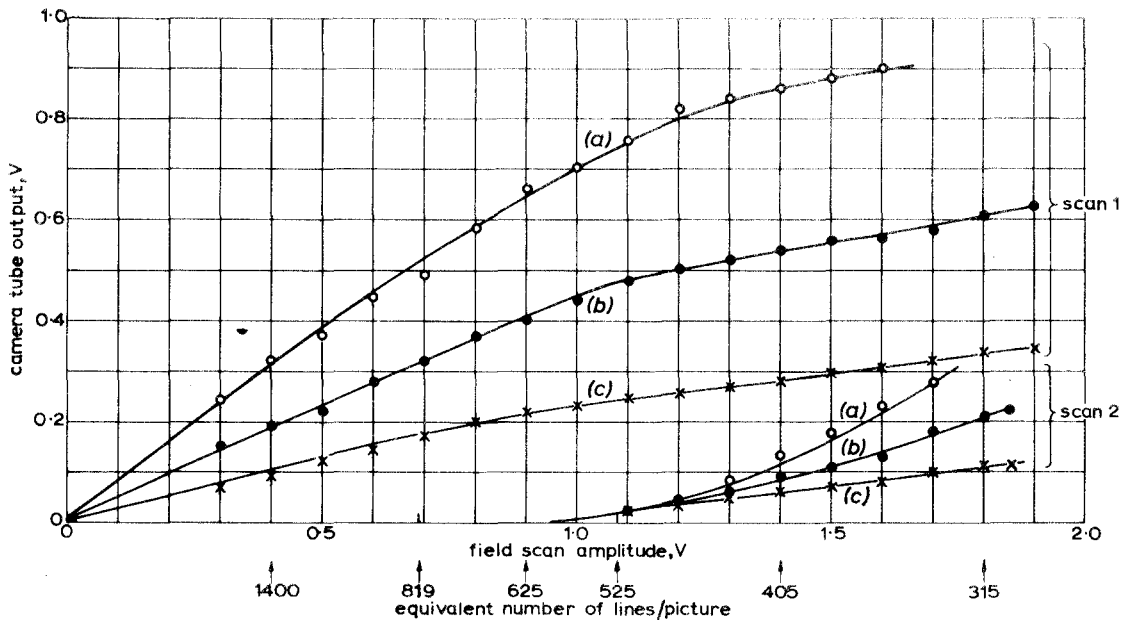


Fig. 20 - The effect of line spacing on the discharge of the target. Scan 1 and scan 2 outputs

- (a) Photocathode illumination  $0.35 \text{ lm/ft}^2$
- (b) Photocathode illumination  $0.022 \text{ lm/ft}^2$
- (c) Photocathode illumination  $0.012 \text{ lm/ft}^2$

From Fig. 21 it will be seen that, for line spacings below that equivalent to 625 lines, per picture height, the ratio  $I_2/I_1$  was zero, but above this number, it increased nearly linearly until the widest spacing measured, corresponding to 315 lines per picture height, was reached. It will be seen from Fig. 22, obtained using 135-line scanning, that the ratio  $I_2/I_1$  increased less rapidly as the spacing increased beyond that corresponding to 250 lines per picture height and as the ideal ratio of 1.0 was approached. The highest value recorded was 0.9, at which point the ratio increased very slowly.

The significance of these measurements may be explained in terms of the following simplified argument; a more detailed treatment is given in Appendix 1.

If the scanning process were perfect, the beam, during each line scan, would deposit charge on the target in a strip of uniform density, whose width is equal to the picture line spacing. If the potential of this strip of the target were to be reduced to the value that just prevents the landing of further beam electrons, the beam would have to deposit, on the strip, a negative charge numerically greater than the positive charge on the corresponding strip of the same size on the image side of the target; this would occur because there are lateral capacitive coupling effects between the strips on the image side of the target. If there were no lateral conduction of charge on the target (an 'ideal' target), this would result in a surplus of negative charge on the scanned strips after neutralization of the positive charge had taken place. This surplus of negative charge would lower the potential of the spaces between the scanned strips of one field scan, again by lateral capacitive



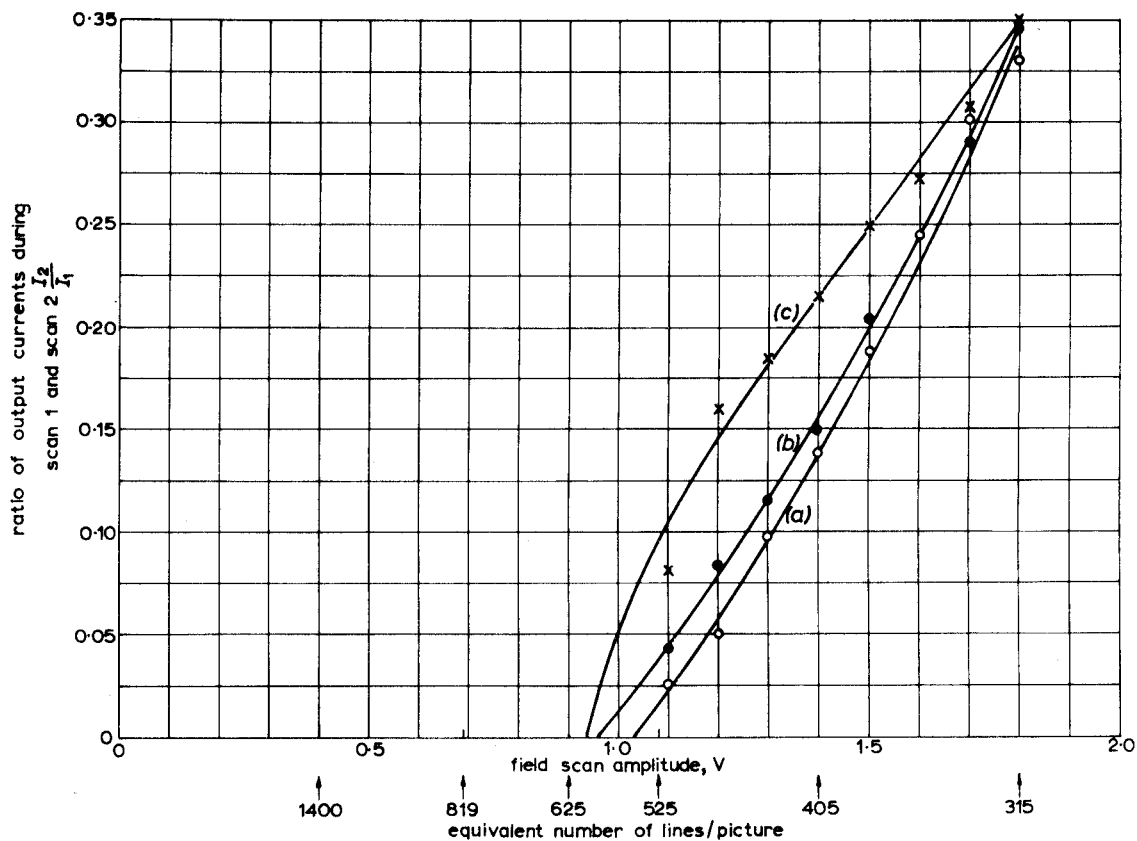


Fig. 21 - The effect of line spacing on the discharge of the target. The ratio of outputs during scan 1 and scan 2

(a) Photocathode illumination 0.022 lm/ft<sup>2</sup> (b) Photocathode illumination 0.012 lm/ft<sup>2</sup>  
 (c) Photocathode illumination 0.012 lm/ft<sup>2</sup>

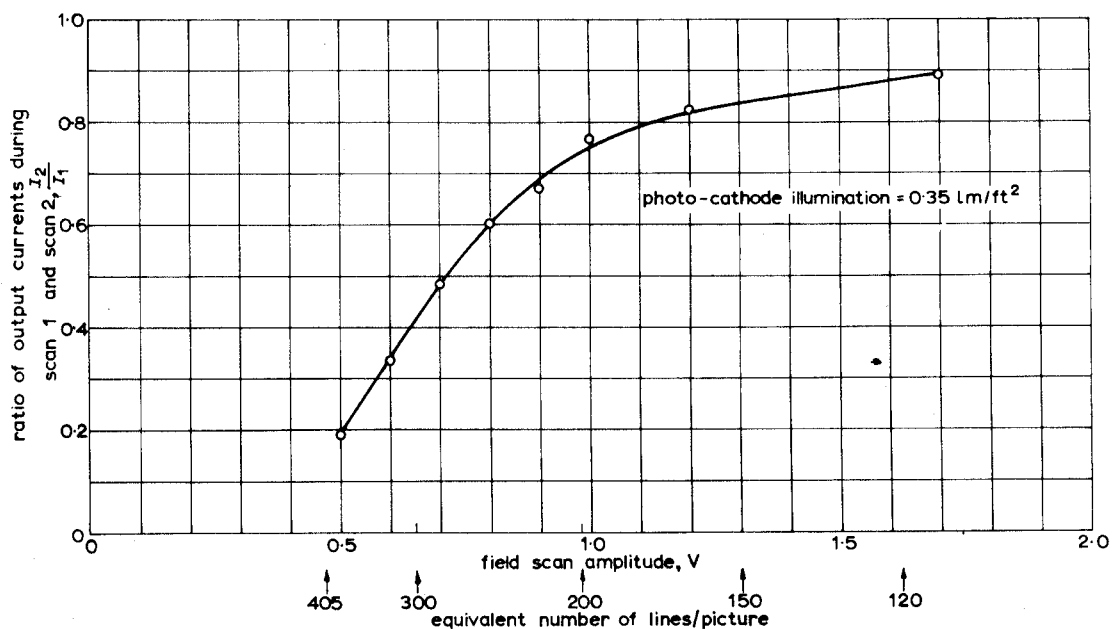


Fig. 22 - The effect of line spacing on the discharge of the target. Ratio of outputs during scan 1 and scan 2 for greatly increased line spacing

coupling, so that, during the ensuing field scan, less negative charge from the beam would be required in order to reduce the target potential to the value at which the beam electrons are rejected. Thus, even under ideal conditions of beam width and target conduction, the ratio  $I_2/I_1$  may be expected to be less than unity.

Two conclusions may be drawn from the measurements:

(i) The beam width is such that, with more than 300 lines in any one field scan, no undischarged target area remains after one field scan. This indicates that the width of the scanning spot measured between the half-amplitude points of its vertical 'profile' is approximately 1/300 of picture height; the profile is considered to be a graph relating to the effectiveness (in terms of discharging the target) of a small filament of the beam to its distance from the beam axis. It is felt, however, that no reliable deduction of the exact shape of the vertical profile can be made from the measurements.

(ii) Even under idealized conditions, the scanning of one field of an interlaced raster affects the scanning of the ensuing field; this is caused by capacitive coupling between elements of the target and lateral leakage in the target.

## 6. THE PORTRAYAL OF A MOVING OBJECT

The apparatus described in Section 3 was used for this experiment by coupling the second disk (shown in Fig. 10(c)) to the shaft. The clear arc of this disk was cut so that its long sides were equiangular spirals

$$r_1 = a\theta + b_1$$

$$\text{and } r_2 = a\theta + b_2$$

and the ends lay along radii of the disk, the angle between them being approximately  $70^\circ$ . The parameters of the long sides of the spiral were chosen so that the radius of the outer side of the slot at any angle  $\theta$  (radians) was equal to that of the inner side of the slot at the angle  $(\theta + \pi/3)$  radians and was a constant amount  $(b_2 - b_1)$  greater than the radius of the inner side of the slot at an angle  $\theta$ . The value of  $a$  is thus given by:

$$a\theta + b_2 = a(\theta + \pi/3) + b_1$$

therefore

$$a = 3/\pi (b_2 - b_1)$$

As seen by the camera, the combined effect of the disks and the fixed defining slot was to produce a sheared rectangular area which moved horizontally at a uniform speed. It was illuminated for slightly less than 1/25th of a second (1/6th of the period of rotation of the disks) during which time it moved a distance equal to its own length.

The camera field-scan phasing was adjusted so that the target area corresponding to the illuminated patch was scanned, (a) immediately before the start of illumination, (b) half-way through the duration of the illumination, and (c) immediately after illumination ceased; scanning then continued for nine more scans before

the cycle was repeated. Fig. 23(a) shows the line waveform of the output signal that would have been produced by a perfect camera on the first three scans after the start of illumination. (The outputs on the next nine scans would be zero).

The output on the first of the three lines would be produced by the integrated effect of the illuminated patch, which had moved a distance equal to one half of its length during this interval of  $1/50$ th of a second. The output on the second scan would be produced by a line of the interlaced field and is assumed to be completely independent of the scanning of the previous field. This output would be the effect of the illuminated patch integrated over the  $1/25$ th of a second that had expired since this line was previously scanned: throughout this time the patch would have been illuminated and would have moved a distance equal to its own length. The output on the third scan would have been due to a line of the original field: because the erasure of the camera is assumed to be perfect, this output would be the effect of the illuminated patch integrated over the second half of the time during which the illumination was present.

These ideal waveforms were based on the following assumptions, none of which are valid:

- (1) the contrast law is linear;
- (2) the integration of charge is perfect;
- (3) there is complete independence of the odd and even scans;
- (4) erasure is complete.

Fig. 23(b) shows diagrammatically the type of waveform obtained in practice. The output on the first scan is larger than would be obtained under idealized conditions, because more than half of the total charge is removed. The output on the second scan may be considered in four parts. The section OG of the graph is produced by the scanning of an area that has already been scanned by one (interlaced) field which has occurred since illumination of that area ceased, so that this part of the waveform is similar in shape to the corresponding part of the first-scan waveform but has only about 20% of its amplitude. The sections GC, CA are the results of scanning combinations of the charge due to part of the illuminated area, integrated over a

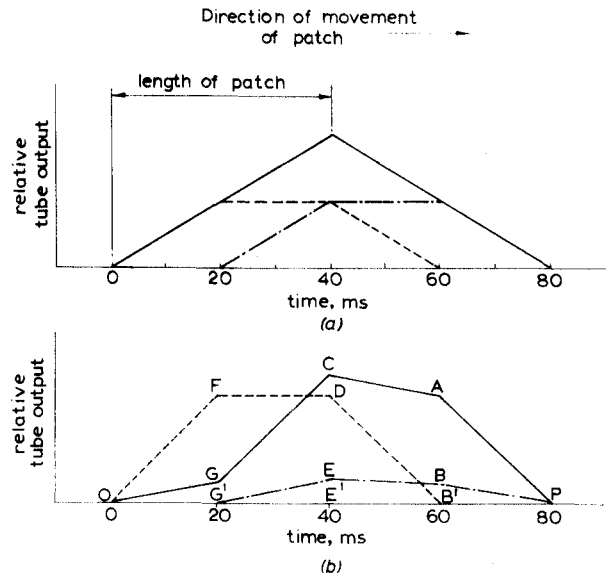


Fig. 23 - Idealized waveforms of moving object experiment

- (a) Idealized camera tube  
(b) Approximation to practical camera tube

----- First scan  
———— Second scan  
- · - · - Third scan

field, with the charge remaining after the first scan: they have been treated as the sum of two components, one of the same shape and in the same position as the first-scan output (but at reduced amplitude) and the other with the same shape and amplitude as the first-scan output but displaced horizontally by half the patch width. The third scan waveform is assumed to remove the remainder of the charge, so that the sum of the waveforms of Fig. 23(b) is the same as the sum of the waveforms of Fig. 23(a).

Photographs of waveforms obtained in practical tests are given in Fig. 24. It will be seen that the results obtained at a medium light level (0.045 ft-C) are very similar to the curve shown in Fig. 23(b). At lower light levels, more independence between scans becomes evident; this may be recognized by the more triangular shape of the second scan and the relative magnitudes of the outputs during scan 1 and scan 2. At higher light levels, the non-linear contrast law becomes apparent; this is particularly noticeable as a curvature in that section of the waveform corresponding to OF in Fig. 23. At the highest illumination, severe white crushing and charge redistribution occur since the tube is then working approximately  $2\frac{1}{2}$  stops over the 'knee' of the contrast law.

In order to confirm that the portrayal of a moving object could be deduced from static measurements, the camera was exposed to a uniformly illuminated area whose brightness could be adjusted, and curves of camera output against illumination were plotted for scan 1 and scan 2 when the exposure was 0.9 of a field and for scans 1, 2 and 3 when the exposure was 1.9 of a field. The outputs corresponding to the exposure conditions of the labelled points of Fig. 23(b) were read off these camera characteristics and were plotted in Fig. 25, together with the corresponding values measured on the oscilloscope traces (Fig. 24).

The points calculated and also measured have been joined in the diagram of Fig. 25 by straight lines and, therefore, Fig. 25 does not show the shapes of the photographed waveforms in Fig. 24. It will be seen that there is good agreement between the measured and calculated points, and that at the lower light level, where the contrast law becomes linear, the photographs and the predicted waveforms (Fig. 25) are very similar indeed. The most surprising aspect of the measurement was that the outputs measured at points of the waveforms corresponding to E in Fig. 23 were consistently lower than those measured at points of the waveforms corresponding to B.

The implication of this is that if the sequence of illumination and scanning is as shown in Fig. 26(a), then there will be a larger output on the second scan after illumination has ceased (scan 2) than there is when the sequence of illumination and scanning is as shown in Fig. 26(b) in which the second scan after illumination has ceased is shown as scan 3. This was checked using stationary patches illuminated for 18 ms and 38 ms, and phased as shown in Fig. 26. This experiment produced the same result and proved that the effect was not fundamentally associated with the fact that the object was moving. Discussion of the possible cause of this effect will be found in the latter part of Appendix 1.

It may be seen that on the 405-line system with illumination corresponding to the region of the knee (0.065 ft-C) of the contrast law, the exposure time of the tube is substantially 1/50 second, there being only 25% of the signal due to the previous 1/50 second exposure present. At lower levels of illumination (0.012 ft-C), the contribution from the previous 1/50 second rises to 40%, so that the exposure time could be said in this case to approach 1/25 of a second.

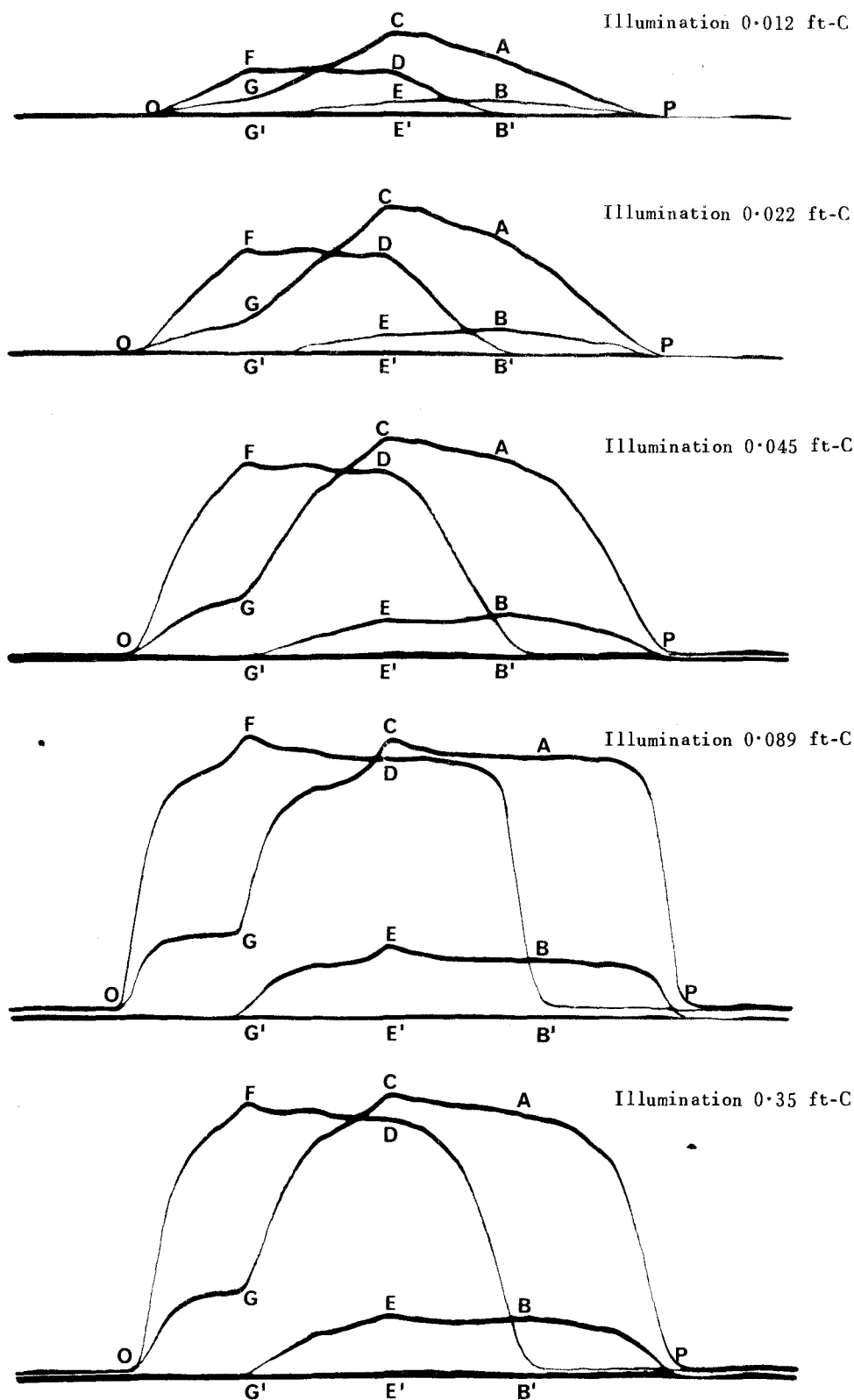


Fig. 24 - Photographed waveforms of moving object experiment

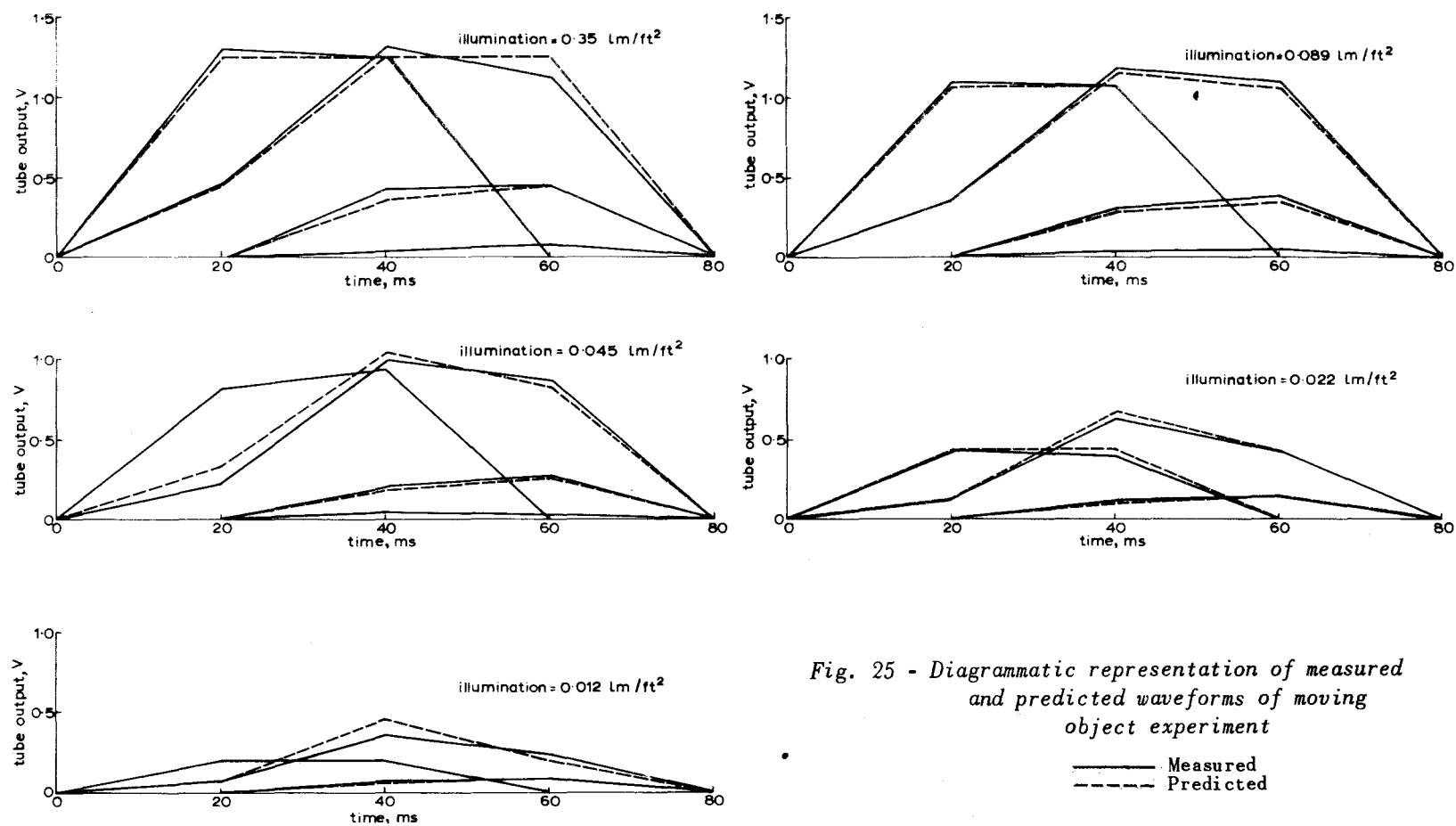


Fig. 25 - Diagrammatic representation of measured and predicted waveforms of moving object experiment

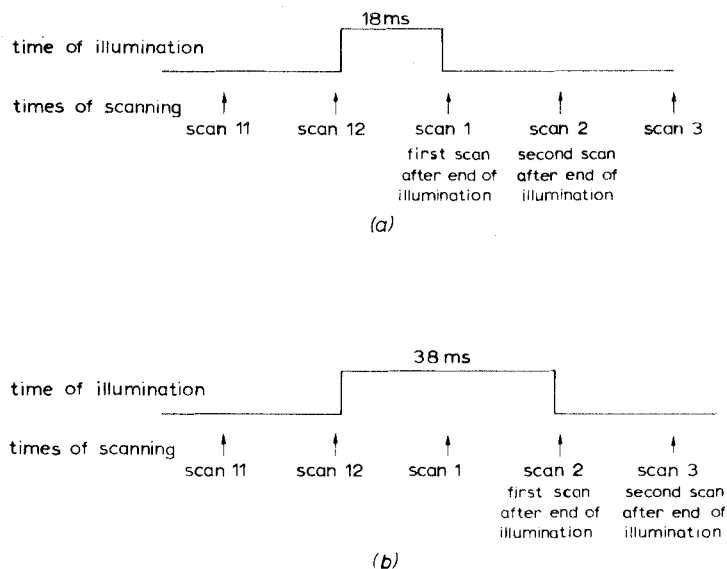


Fig. 26 - Illumination periods of one field and two fields duration

- (a) One field
- (b) Two fields

At illumination levels in the region of  $1/2$  stop above the knee ( $0.089$  ft-C) the exposure time may be considered to be less than  $1/50$  second, since in the first  $1/100$  second the output obtained is 88% of that achieved after  $1/50$  second. The edges of moving objects will thus be portrayed as if the exposure were  $1/100$  second, but the length of the object will apparently be increased to show the total distance travelled in  $1/50$  second.

Measurements already described indicate that the effective exposure time of  $1/50$  second is maintained to a lower light level on 525-line and 625-line systems due to the more complete erasure of adjacent lines resulting from the closer line spacing on these systems.

## 7. CONCLUSIONS

The characteristics of target discharge are dependent on a large number of factors, the most important of which are accuracy of beam focus, beam current, target temperature, illumination and scanning standard.

De-focusing of the beam produces more complete erasure of the target during one scan, resulting in less independence between odd and even scans. Beam current affects the degree of erasure to a small extent, high values of beam current increasing the amount of erasure during one scan.

Target temperature affects erasure appreciably at illumination levels one stop below the knee. At temperatures less than the working temperature of  $45^{\circ}\text{C}$  the reduced lateral leakage allows a signal of 50% of the first scan signal to be read off during the second scan, rather than the usual value of 20% to 25% (405-line

system). At levels of illumination higher and lower than the preferred operating point, there is less dependence on temperature.

The dependence on illumination level is such that the degree of discharge of the target is constant at or above, the knee of the contrast law. As the light level is reduced below that corresponding to the knee, the degree of target discharge of the target is constant at or above, the knee of the contrast law. As the light level is reduced below that corresponding to the knee, the degree of target discharge is reduced until, at an illumination level of one tenth that corresponding to the knee, the output obtained during the second scan is half that obtained during the first.

The scanning standard in use has a large influence on target discharge. With the 405-line standard and a light level at, or above, the knee the ratio  $I_2/I_1$  was 0.20 to 0.25. As the number of scanning lines is increased, this ratio becomes smaller, until, for 625 lines, it is less than 0.05 and, for 819 lines, it is immeasurably small.

The portrayal of a moving object is influenced by all the factors which can change the ratio  $I_2/I_1$ . Any factor which increases this ratio will increase the exposure time; conversely, any factor which reduces it, will reduce the exposure time to a minimum value of 1/50 second. Exposure above the knee increases the definition of edges of a moving object (to that corresponding to 1/100 second exposure) but the object will appear unnaturally long since the exposure can never be for less than a field period. The use of illumination in the region of the knee, a target temperature of 45°C and adequate beam current are all required for the best portrayal of motion.

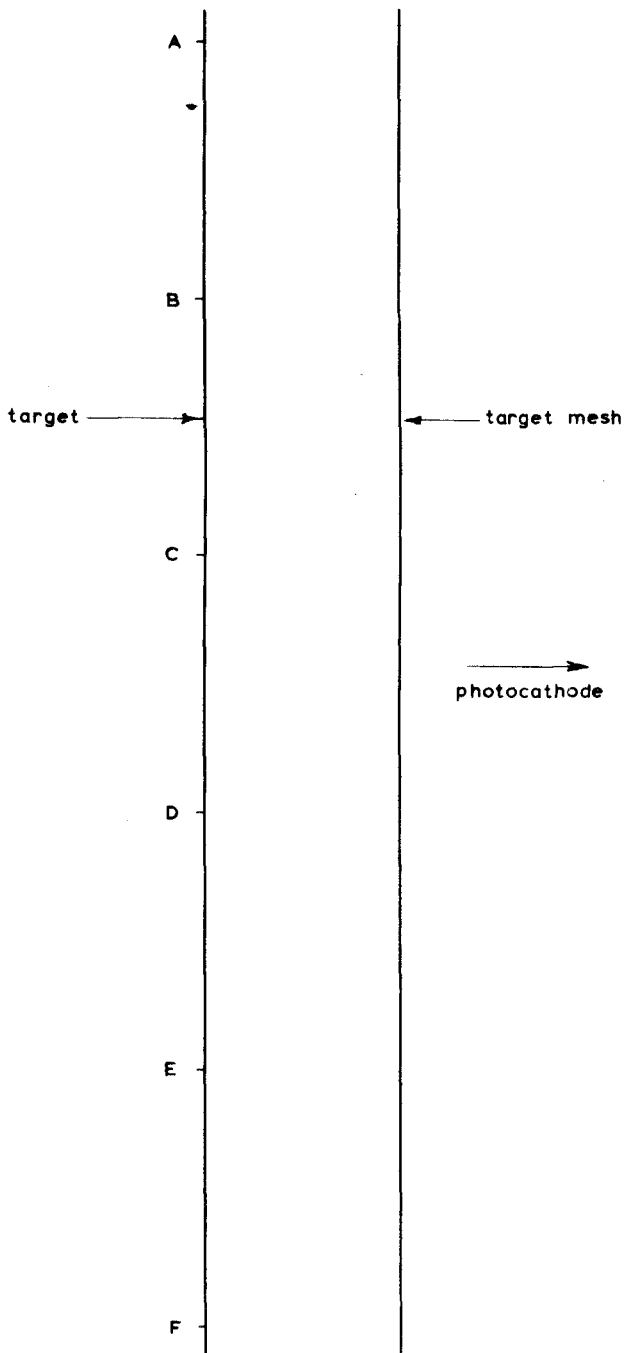
## 8. REFERENCES

1. 'Image Orthicon Investigations : The Measurement of Currents Within the Tube', Research Department Report No. T-100, Serial No. 1963/2.
2. 'Image Orthicon Investigations : The Local Effects of Small Area Highlights', Research Department Report No. T-100/2, Serial No. 1963/4.
3. Rotow, A.A., 'Image Orthicon for Pick-up at Low Light Levels', R.C.A. Review, September 1956, pp. 425 - 435.
4. Janes, R.B., and Rotow, A.A., 'Light Transfer Characteristics of Image Orthicons', R.C.A. Review, September 1950, pp. 364 - 376.
5. Meltzer, B., and Holmes, P.L., 'Beam Temperature Discharge Lag and Target Biasing in Some Television Pick-up Tubes', Brit. J. App. Phys., No. 9, April 1958, pp. 139 - 143.
6. McGee, J.D., 'A Review of Some Television Pick-up Tubes', Proc. I.E.E., Part III, November 1950, pp. 377 - 392.
7. Janes, R.B., Johnson, R.E., and Moore, R.S., 'Development and Performance of Television Camera Tubes', R.C.A. Review, Vol. 10, No. 2, June 1949, pp. 191 - 223.



8. 'Image Orthicon Investigations : Vertical Resolution', Research Department Report No. T-100/5 in preparation.
9. 'A Test Bench for  $4\frac{1}{2}$  in Image Orthicons', Research Department Technical Memorandum No. T-1045.
10. Black, K.G., and Higgins, T., 'Rigorous Determination of the Parameters of Microstrip Lines', Trans. I.R.E., M.T.T.-3, No. 2, 1955, p. 85.

## APPENDIX 1

*The Theoretical Value of  $I_2$  to  $I_1$* 

It has been shown in Section 2 that there are field shading components in the scan-1 and scan-2 outputs when scanning the charged area corresponding to a bright patch in the scene, especially when the scanning spot is wide. If the patch is large enough to occupy many scanning lines, e.g. with a height equal to one quarter of the picture height, and if the spot is small, there will be little shading over the centre part of the area. If it were possible to illuminate the whole target uniformly there would be virtually no shading at the centre.

The ratio of the scan-2 to scan-1 outputs,  $I_2/I_1$ , has been estimated by three methods:

- (i) by calculations of electrostatic capacitance;
- (ii) by use of a conductive sheet analogue;
- (iii) by a numerical computation.

The results of the first two are in close agreement with each other but because of the approximations which are inherent in the methods, the results indicate too low a value for  $I_2/I_1$ .

The result of the third method, which does not take lateral leakage of the target into account, is consistent with the results measured at low temperature.

Fig. 27 represents a section of the tube showing the target and the target mesh, the spacing between them being

Fig. 27 - Vertical section through the target and its mesh

approximately  $1.5 \times 10^{-3}$  in ( $3.8 \times 10^{-2}$  mm). With the 405-line system, the pitch of the picture lines is approximately  $4 \times 10^{-3}$  in (0.1 mm); under ideal conditions the beam would discharge alternate strips of the target during one field and discharge the interlacing strips during the next field. If the photo-cathode were illuminated evenly, there would be a uniform charge on the target which would then be at uniform potential, apart from the effects of the variation in the capacitance per unit area between the surface of the target and other electrodes of the tube.

Assume that the scanning beam is switched off while the illumination is present and that scanning starts immediately after the illumination is switched off. Let AB in Fig. 27 represent the vertical width of one line of the scan. If the scanning beam is exactly one line pitch in diameter and it is fully effective in discharging the target, sufficient negative charge will be placed on AB to reduce its potential to that of the cathode. When the next line of the field, CD, is scanned, the beam will find that the potential of CD has already been reduced to some extent by the discharge of AB and so less negative charge will be required on CD to bring it to cathode potential. The condition when EF is scanned will only be slightly different; AB is sufficiently remote to have little effect.

During the remainder of the field scan, the charge deposited will be neutralized by some of the positive charge on the image-section side of the target. When the following (interlaced) field scans the line BC, it will find that the potential there is much lower than the potential of CD had been during the previous field (i.e. just after AB was scanned). The charge required to bring BC to cathode potential would therefore be less than that required for the line CD during the first scan. The conditions applying when DE is scanned will be very similar to those when BC is scanned.

#### *Estimate of $I_2/I_1$ from Capacitance Calculations*

It is possible to find the ratio of  $I_2$  to  $I_1$  from the calculation of capacitances, if it is assumed that the effect of the line AB on the next line in the same field, CD, may be neglected.

Let  $C'$  be the 'small area' capacitance per unit length of line scan between CD (assumed to be at uniform potential) and the target mesh. If  $\Delta V$  is the change of voltage of CD during discharge, the quantity of charge required is  $C'\Delta V$ .

Let  $C_1$  be the capacitance per unit length of line scan from CD to an equally wide strip of target mesh, assuming that there is no fringing of the lines of the electrostatic field (i.e., if the whole of the target plane were at the potential of CD).

If the whole target were discharged, the quantity of charge required per picture line would be  $C_1\Delta V$ , so two adjacent lines of a picture would require  $2C_1\Delta V$ . The charge deposited on one line during the first field is  $C'\Delta V$ , so that required in the scan of the second line is given as  $2C_1\Delta V - C'\Delta V$ ; this point is further discussed later in this Appendix. The ratio, scan-2 output to scan-1 output would then be:

$$\frac{2C_1\Delta V - C'\Delta V}{C'\Delta V} = \frac{2 - C'/C_1}{C'/C_1}$$

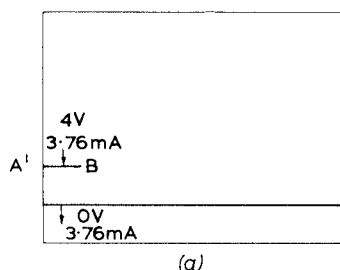
From a paper by Black and Higgins<sup>10</sup> the ratio  $C'/C_1$  is approximately 1.8 giving a ratio

$$I_2 = \frac{2 - 1.8}{1.8}$$

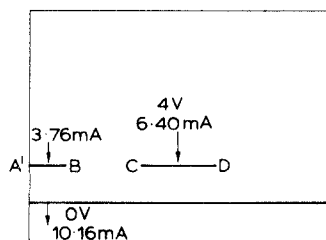
$$I_1 = 0.11$$

### Estimate of $I_2/I_1$ from Conductance-Sheet Analogue

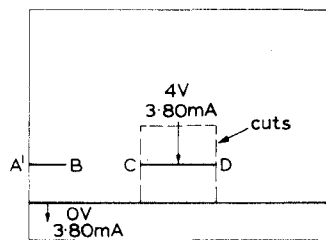
The electrostatic field between a line of charge on the target and the uniform potential target mesh can be represented by an analogue consisting of a conductive medium such as an electrolytic tank, conductive paper or a mesh of resistors. Electrodes with very high conductivity are connected to the analogue to represent equipotential surfaces in the original and potentials are applied to them representing the corresponding voltages in the original. The equipotential contours in the original and the analogue correspond directly and the charges in the original are represented by the currents in the electrodes of the analogue. The analogue used for this estimate was a sheet of 'Teledeltos' paper that had a lateral resistance of approximately 2000 ohms per square. Conductive lines were deposited by painting with silver paint.



(a)



(b)



(c)

Fig. 28 - Measurements on conductance-sheet analogue representing interlaced scanning

- Boundary of and cuts in the conducting sheet
- ⊥ Electrodes with current connections

- (a) First stage of measurement
- (b) Second stage of measurement
- (c) Third stage of measurement

On the sheet of 'Teledeltos' paper two lines were deposited, one representing the target mesh and the other representing approximately one half (A'B) of AB, Fig. 28(a). The other half of AB was omitted, the part drawn being taken to the edge of the sheet as an economy in time and materials which would not make any appreciable difference to the accuracy of the result.

A potential difference of 4 V was applied between the lines and the current was found to be 3.76 mA.

A conductive line was then deposited to represent CD, Fig. 28(b). When the voltage from CD to the target mesh was 4 V and the current in A'B was again made 3.76 mA, it was found that the current in CD was 6.40 mA.

The paper was then cut along two lines through the ends of CD, perpendicular to it and to the target mesh, the cuts extending from the mesh to the opposite side of CD. A third cut was made joining the other two on the side of CD remote from the mesh (Fig. 28(c)). When 4 V was applied between CD and the target mesh, the current was found to be 3.80 mA.

Before scanning, the positive charges on BC and CD would each be represented by 3.80 mA, so their sum would be represented by 7.60 mA.

The negative charge deposited on CD during scan 1 would be represented by 6.40 mA.

The charge remaining on BC and CD for discharge during scan 2 would therefore be represented by  $7.6 - 6.4 = 1.2$  mA

$$\begin{aligned} \text{therefore} \quad \frac{I_2}{I_1} &= \frac{1.2}{6.4} \\ &= 0.19 \end{aligned}$$

#### Comparison between the Results of the Two Methods

In the first method of estimating the ratio  $I_2$  to  $I_1$ , the effect of the charge on AB upon the charge taken by CD was neglected. As a result, the 'scan-1' value is a little too high, and the ratio is a little low.

In the second method, when the equipment was set up as in Fig. 28(b), the section A'B of the analogue is at a uniform potential because of the conducting material of the electrode. In the practical case there is a potential gradient along AB when the charge is applied to CD: the potential at B in the analogue is too low, and, therefore, the current in CD is too high, so the estimated value of the ratio is again low. The mean of the two values obtained is:

$$\frac{1}{2} (0.11 + 0.19) = 0.15$$

#### *Estimate of the Ratio of $I_2$ to $I_1$ from an Approximate Computation*

It has been assumed in the first part of this Appendix that the charge deposited by the beam during scan 2 would be that required to give a total negative charge on the target equal to the original positive charge. A more realistic assumption would be that during scan 2 the appropriate parts of the target are brought to cathode potential; as a result, the scanning lines of the first field will, in fact, be driven somewhat negative with respect to the cathode. The total negative charge deposited is greater than the original positive charge, and the estimates of the ratio in the previous sections are therefore too small. Under normal operating conditions and with continuous illumination, only a few scans are required to bring the target to a condition in which the positive and negative swings of target potential, relative to the mesh, are such that the negative charge lost as secondary emission is balanced by that collected from the beam.

Although the method to be described involves many approximations, the results are in good qualitative agreement with observations on practical tubes and the numerical results are close to the measured values. During the measurements on the conductance-sheet analogue it was estimated that, if one line of the raster on the target were held at a uniform potential, the mean potential across the adjacent (interlaced) line would be approximately 0.2 of the potential on the charged line. An error in this figure would change the numerical results of the present method without materially altering the qualitative results.

Assume that the small-area capacitance per unit length of one scanned line is unity; the units of potential and charge are arbitrary, linked only by the assumed unit of capacitance. For a longitudinal section of the camera tube, through the target, it is possible to tabulate the assumed mean potentials of various scanning lines caused by a unit charge on one of them (Table 1).

TABLE 1

*The assumed distribution of potential due to one charged line*

Charge	0	0	0	0	1	0	0	0	0
Assumed potential	·0016	·0080	·0400	·2000	1·0000	·2000	·0400	·0080	·0016

If three adjacent scanning lines are charged, the result is as shown in Table 2. The sums of these potentials give the resulting field due to the distributed charge.

TABLE 2

*The distribution of potential due to three charged lines*

Charges	0	0	0	1	1	1	0	0	0
Potential due to 1st charge	·0080	·0400	·2000	1·0000	·2000	·0400	·0080	·0016	·0003
Potential due to 2nd charge	·0016	·0080	·0400	·2000	1·0000	·2000	·0400	·0080	·0016
Potential due to 3rd charge	·0003	·0016	·0080	·0400	·2000	1·0000	·2000	·0400	·0080
Sums	·0099	·0496	·2480	1·2400	1·4000	1·2400	·2480	·0496	·0099

Such a tabulation was completed assuming that there were nineteen charged lines; the charge and potential distribution patterns are shown in Fig. 29, which should be compared with Fig. 2(b). The figures for the first seven values of the potential distribution are shown in the top line of Table 3.

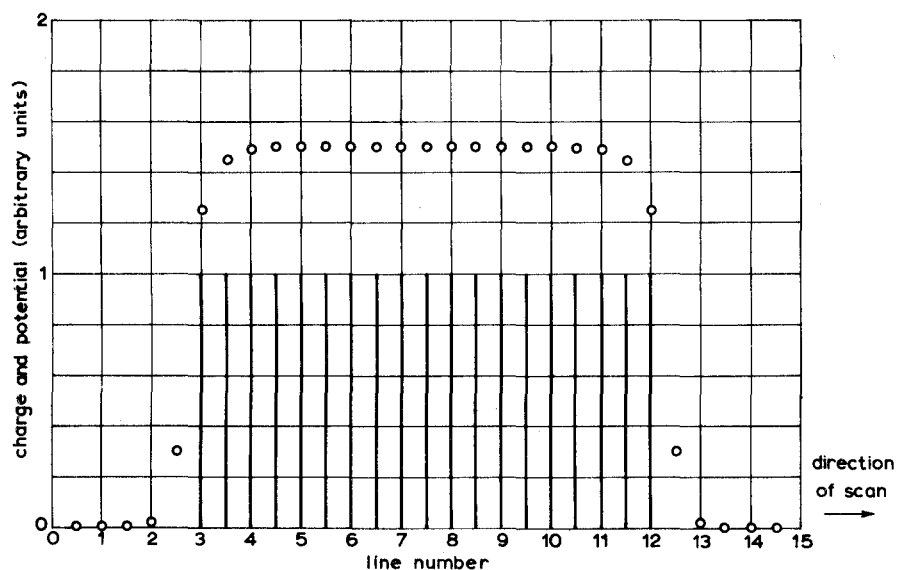


Fig. 29 - Charge and potential distributions (computed)

| Lines carrying unit charge  
 ○ ○ ○ Potential of the target (computed)

When the beam scans the first line for which the potential is tabulated, it will deposit  $\cdot 00002$  units of negative charge. The effects of this on the other lines will be negligibly small. When the next line of the same field is scanned, it will receive  $\cdot 00040$  units of negative charge. The potential distribution due to this charge is written down and subtracted from the original distribution, (lines 4 and 5 of Table 3).

Similarly, the third line of scanning will deposit  $\cdot 00998$  units of charge; its potential distribution is written down and subtracted, as shown in lines 6 and 7 of Table 3.

TABLE 3

*The first three lines of scan potential distributions*

At start	$\cdot 00002$	$\cdot 00008$	$\cdot 00040$	$\cdot 00200$	$\cdot 01000$	$\cdot 05000$	$\cdot 25000$	etc.
Potentials due to charge on line 1	$\cdot 00002$	nil	nil	nil	nil	nil	nil	
After line 1	nil	$\cdot 00008$	$\cdot 00040$	$\cdot 00200$	$\cdot 01000$	$\cdot 05000$	$\cdot 25000$	
Potentials due to charge on line 2	$\cdot 00002$	$\cdot 00008$	$\cdot 00040$	$\cdot 00008$	$\cdot 00002$	nil	nil	
After line 2	$-\cdot 00002$	nil	nil	$\cdot 00192$	$\cdot 00998$	$\cdot 05000$	$\cdot 25000$	
Potentials due to charge on line 3	$\cdot 00002$	$\cdot 00008$	$\cdot 00040$	$\cdot 00200$	$\cdot 00998$	$\cdot 00200$	$\cdot 00004$	
After line 3	$-\cdot 00004$	$-\cdot 00008$	$-\cdot 00040$	$-\cdot 00008$	nil	$\cdot 04800$	$\cdot 26996$	
Charges deposited	$\cdot 00002$		$\cdot 00040$		$\cdot 00998$			

The process was continued for 14 lines through the region which started at a positive potential; the charge deposited on each line is shown in Fig. 30.

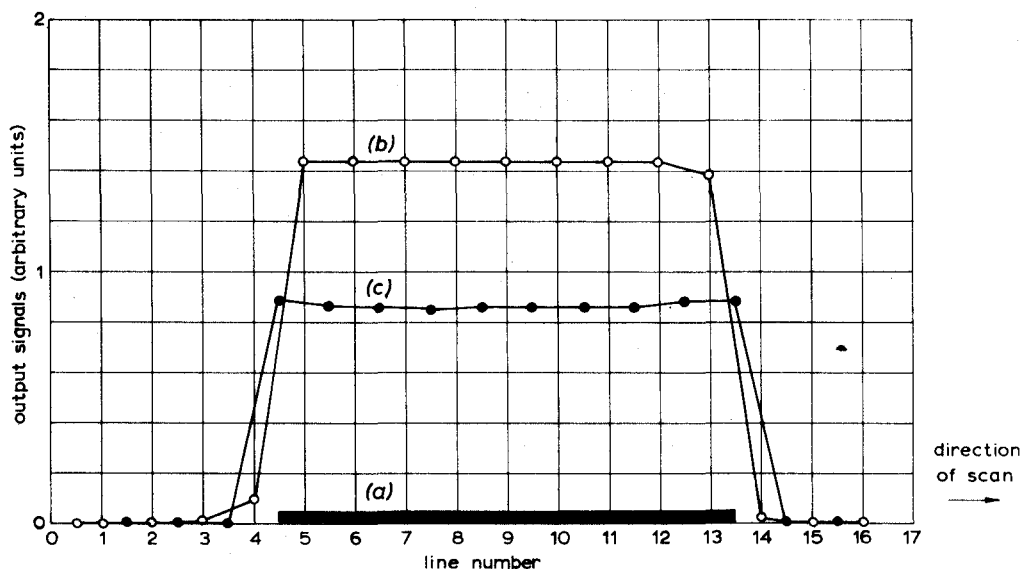


Fig. 30 - Outputs during scan 1 and scan 2 (computed)

- (a) Lines initially charged
- (b) Outputs during scan 1
- (c) Outputs during scan 2

The next field scans the interlacing lines. If there is no further illumination after the first scan, the final potential distribution after scan 1 is the initial distribution for scan 2 (apart from the effects of leakage in the target which is neglected in this analysis). The computation was repeated and the scan-2 outputs which were deduced are also shown in Fig. 30.

From the figure, the ratio of  $I_2$  to  $I_1$  is  $0.86/1.44 = 0.6$ , which agrees closely with the measured values found when the target was cold and there was little lateral leakage.

If there were a second field of exposure, the potential distribution at the start of the second scan of the charged area would be found by adding, to the potential remaining after scan 1, a potential distribution equal to that due to the original positive charge distribution. This was done, and the computation repeated. The mean level of the outputs on scan 2 was found to be 2.30. It was then assumed that there was a third scan with no further illumination and the mean output was found to be 0.46. This is lower than the scan 2 output for a single field exposure, which is qualitatively consistent with measured results (see Section 6 of this report).

The quantitative results cannot be compared directly because the computation neglected lateral leakage in the target, which is known to be significant at the temperatures at which the measurement was made.



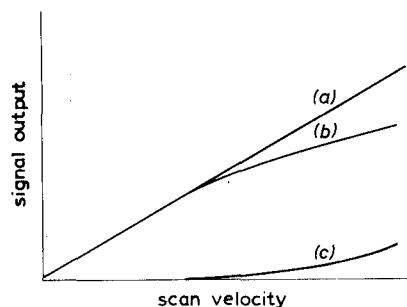
## APPENDIX 2

*The Effect of a Change in Line-Scan Velocity on the Discharge of the Target*

Fig. 5 shows the output from the tube on three successive scans, found by marking off three equal areas  $A = T/C$  under the graph of the reciprocal of target current against target voltage. If the line scan velocity is increased, the ratio  $T/C$  will be reduced since a given target area will be scanned in a shorter time, so  $S_1$ , which is proportional to the charge deposited by the first scan, will also be reduced. If the quantity of charge read off a given area had been constant, the signal current from the tube would have been proportional to the rate at which the charge was collected by the target from the beam, so the graph of output against scan velocity would be a straight line through the origin. It has been shown that, in a practical tube, the charge collected from a given area falls off as the velocity increases, so the rate of increase of signal current is less rapid than the rate of increase in velocity; thus the graph of the scan-1 output against scan velocity will be concave downwards as shown in Fig. 31, curve (b).

Fig. 31 - The variation of signal output with line scan velocity

- (a) Ideal output from scan 1
- (b) Effect of beam characteristics on scan 1 output
- (c) Scan 2 output



As the scan velocity is changed, there will be two influences on the output on scan 2. It is seen from Fig. 5 that:

- (i) the reduction in  $A = T/C$  will tend to reduce  $S_2$ ;
- (ii) because  $S_1$  has been reduced, the upper boundary of  $S_2$  will be moved to a higher voltage. The mean value of  $1/i$  is reduced, which tends to increase  $S_2$ .

Under normal conditions, the second of these factors has the greater effect. The increase in scan-2 output will be more than proportional to the increase in scan velocity and the graph of output against velocity will be concave upwards (Fig. 31, curve (c)). The ratio of  $I_2$  to  $I_1$  will therefore increase as the scan velocity increases.

These curves agree with the results of Section 5.7.

